

**ESTIMATION OF HOLE CLEANING CONDITION IN  
REAL-TIME WHILE DRILLING (OPERATIONAL  
POINT OF VIEW)**

**BY**

**Mahmoud Nader M. Elzenary**

**A Thesis Presented to the  
DEANSHIP OF GRADUATE STUDIES**

**KING FAHD UNIVERSITY OF PETROLEUM & MINERALS  
DHAHRAN, SAUDI ARABIA**

**In Partial Fulfillment of the  
Requirements for the Degree of**

**MASTER OF SCIENCE**

**In**

**PETROLEUM ENGINEERING**

**January, 2019**

KING FAHD UNIVERSITY OF PETROLEUM & MINERALS

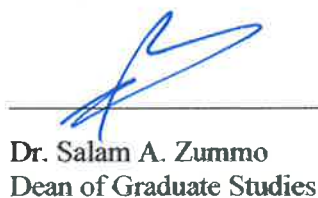
DHAHRAN- 31261, SAUDI ARABIA

**DEANSHIP OF GRADUATE STUDIES**

This thesis, written by **Mahmoud Nader M. Elzenary** under the direction of his thesis advisor and approved by his thesis committee, has been presented and accepted by the Dean of Graduate Studies, in partial fulfillment of the requirements for the degree of **MASTER OF SCIENCE IN PETROLEUM ENGINEERING.**



Dr. Dhafer A. Al Shehri  
Department Chairman



Dr. Salam A. Zummo  
Dean of Graduate Studies



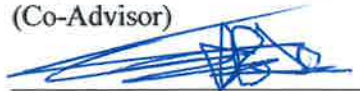
8/11/18  
Date



Dr. Salaheldin M. Elkatatny  
(Advisor)



Dr. Abdulazeez Abdulraheem  
(Co-Advisor)



Dr. Abdulaziz A. Al Majed  
(Member)



Dr. Mohamed Mahmoud  
(Member)



Dr. Shirish Patil  
(Member)

© Mahmoud Nader Mahmoud

2019

*[To my lovely wife and my children Yassein and Ezzeldin without whom this thesis  
would not have been completed ]*

## **ACKNOWLEDGMENTS**

The conclusion of this thesis brings to an end my master's program at King Fahd University of Petroleum and Minerals. It leads to an MSc degree in Petroleum Engineering with specialization in Drilling Engineering.

I am highly indebted to my advisor, Dr. Salaheldin Elkatatny for giving me the chance to work on this stunning thesis work. His immense support and guidance throughout the thesis period are highly appreciated. Most importantly, I appreciate his open-door policy toward me, I was welcomed at any time of the day and days of the week. Sincerely speaking, I wish this work continues in some sort of way because I have in the past six months become an expert in this part of drilling Engineering that is so important to the Petroleum industry.

I will not end this section without thanking my committee members for their support and encouragement.

And finally, to all my friends and course mates in Petroleum Engineering, I wish to say a big thank you.

|

# **TABLE OF CONTENTS**

<b>ACKNOWLEDGMENTS .....</b>	<b>V</b>
<b>TABLE OF CONTENTS.....</b>	<b>VI</b>
<b>LIST OF TABLES.....</b>	<b>IX</b>
<b>LIST OF FIGURES.....</b>	<b>X</b>
<b>LIST OF ABBREVIATIONS.....</b>	<b>XII</b>
<b>ABSTRACT .....</b>	<b>XIII</b>
<b>ملخص الرسالة .....</b>	<b>XV</b>
<b>CHAPTER 1 INTRODUCTION.....</b>	<b>17</b>
<b>1.1 Background .....</b>	<b>17</b>
<b>1.2 Significance, Scope and Definitions .....</b>	<b>20</b>
<b>CHAPTER 2 LITERATURE REVIEW .....</b>	<b>22</b>
<b>2.1 Factors Affecting Hole Cleaning.....</b>	<b>23</b>
<b>2.1.1 Cutting/Particle Size .....</b>	<b>24</b>
<b>2.1.2 Drill Pipe Eccentricity.....</b>	<b>25</b>
<b>2.1.3 Drill Pipe Rotation .....</b>	<b>28</b>
<b>2.1.4 Hole Size and Hole Angle .....</b>	<b>31</b>
<b>2.1.5 Rheology .....</b>	<b>33</b>
<b>2.1.6 Cutting Transport Ratio .....</b>	<b>39</b>
<b>2.1.7 Rate of Penetration .....</b>	<b>42</b>

2.2	FLOW PATTERNS AND FORCES ACTING ON DRILL CUTTINGS .....	44
2.2.1	Flow Patterns .....	44
2.2.2	Forces Acting on a Suspended Drill Cutting.....	45
2.3	Optimum flow rate for hole cleaning while drilling .....	51
2.4	Artificial Intelligence .....	53
2.4.1	Artificial Neural Network (ANN) .....	54
2.4.2	Adaptive Neuro-Fuzzy Inference System (ANFIS) .....	55
2.5	Equivalent Circulating Density (ECD) .....	57
<b>CHAPTER 3 NEW HOLE CLEANING MODEL.....</b>		<b>59</b>
3.1	Methodology .....	59
3.2	Equivalent circulating density (ECD) prediction using Artificial Intelligence (AI).....	63
3.2.1	First ECD Model – ANN: .....	65
3.2.2	Second ECD Model – ANFIS .....	67
3.3	Mud Rheology prediction using Artificial Intelligence .....	69
3.3.1	First Rheological Model – ANN .....	71
3.3.2	Second Rheological Model – ANFIS.....	75
<b>CHAPTER 4 RESULTS AND CONCLUSIONS.....</b>		<b>81</b>
4.1	Hole Cleaning Efficiency (HCI) .....	81
4.1.1	Stage 1 – ECD Prediction.....	83
4.1.2	Stage 2 - Rheological Properties Prediction .....	86
4.1.3	Stage 3 – HCI Model Verification .....	91
4.2	HCI Software .....	94
4.3	Analysis and Limitations .....	96
4.4	Conclusions .....	97

<b>REFERENCES.....</b>	<b>99</b>
<b>VITAE.....</b>	<b>110</b>



## LIST OF TABLES

Table 1 - Sphericity for different cuttings shapes.....	25
Table 2 - Equations for determining flow behavior parameters .....	38
Table 3 - Equations for determining average velocity.....	38
Table 4 - HCI Parameters Identification .....	62
Table 5 - Statistics Analysis of the used data set .....	65
Table 6 - ANN model training and testing Correlation Coefficient and AAPE .....	67
Table 7 - ANFIS model training and testing Correlation Coefficient and AAPE .....	68
Table 8 - Statistics Analysis of the used data set .....	71
Table 9 - ANN rheological model training and testing Correlation Coefficient and AAPE .....	75
Table 10 - ANFIS rheological model training and testing Correlation Coefficient and AAPE .....	80
Table 11 - Part of the Real drilling parameters – Oil well in north Africa .....	82
Table 12 - ECD/ANN model training and testing Correlation Coefficient and AAPE ....	86
Table 13 - ANN & ANFIS rheological models training and testing Correlation Coefficient and AAPE .....	91
Table 14 - HCI model outputs vs 135 depth points.....	93

## LIST OF FIGURES

Figure 1 - Hole cleaning in deviated wells .....	19
Figure 2 - Drilling Fluid movement downhole .....	22
Figure 3 - Key variables controlling cuttings transport .....	24
Figure 4 - Depiction of pipe Eccentricity .....	27
Figure 5 - Pipe rotation helps fluid flow in the narrow side of an eccentric annulus .....	28
Figure 6 - Illustration of wide and narrow sides in an eccentric annulus .....	29
Figure 7 - Effect of drill string rotation on cuttings transport in a horizontal wellbore.....	30
Figure 8 - Effect of drill string rotation on cuttings transport in a wellbore at 65 degrees angle.....	30
Figure 9 - Effect of hole angle on particle sedimentation.....	32
Figure 10 - Effect of inclination angle on the critical velocity .....	33
Figure 11 - Effect of mud flow rate on annular cuttings mass concentration.....	39
Figure 12 - Effect of ROP on the critical velocity.....	43
Figure 13 - Flow patterns for solids/liquid flow in high angle and horizontal annulus....	45
Figure 14 - Streamline of fluid movement about a settling or suspended particle .....	46
Figure 15 - Forces applied to a particle on a solids bed.....	47
Figure 16 - Forces acting on a single particle .....	47
Figure 17 - ANN System .....	55
Figure 18 - Adaptive neuro fuzzy inference system .....	56
Figure 19 - ROP histogram before filtering.....	64
Figure 20 - ROP histogram after filtration.....	64
Figure 21 - Predicted ECD for booth ANN training and testing compared with Field measurement .....	66
Figure 22 - ECD profile of booth ANN model training and testing compared with ECD from field measurement .....	66
Figure 23 - Predicted ECD from ANFI Model (training and testing) compared with field measurement. ....	67
Figure 24 - ECD profile of booth ANFIS model training and testing compared with ECD from field measurement .....	68
Figure 25 - Initial marsh funnel viscosity Histogram .....	70
Figure 26 - Final Marsh funnel viscosity Histogram.....	70
Figure 27 - Predicted YP from ANN Model compared with field measurement (training results).....	72
Figure 28 - Predicted YP from ANN Model compared with field measurement (testing results).....	72
Figure 29 - Predicted PV from ANN Model compared with field measurement (training results).....	73

Figure 30 - Predicted PV from ANN Model compared with field measurement (testing results).....	73
Figure 31 - Predicted AV from ANN Model compared with field measurement (training results).....	74
Figure 32 - Predicted AV from ANN Model compared with field measurement (testing results).....	74
Figure 33 - Predicted YP from ANFIS Model compared with field measurement (training results).....	76
Figure 34 - Predicted YP from ANFIS Model compared with field measurement (testing results).....	76
Figure 35 - Predicted PV from ANFIS Model compared with field measurement (training results).....	77
Figure 36 - Predicted PV from ANFIS Model compared with field measurement (testing results).....	78
Figure 37 - Predicted AV from ANFIS Model compared with field measurement (training results).....	79
Figure 38 - Predicted AV from ANFIS Model compared with field measurement (testing results).....	79
Figure 39 - Predicted ECD from ANN Model compared with field (training) .....	83
Figure 40 - Predicted ECD from ANN Model compared with field (testing) .....	84
Figure 41 - ECD profile of training ANN model compared with ECD from field measurement .....	85
Figure 42 - ECD profile of training ANN model compared with ECD from field measurement .....	85
Figure 43 - Predicted YP from ANFIS Model compared with the field (training).....	87
Figure 44 - Predicted YP from ANFIS Model compared with the field (testing) .....	87
Figure 45 - Predicted PV from ANN Model compared with the field (training) .....	88
Figure 46- Predicted PV from ANN Model compared with the field (testing) .....	89
Figure 47 - Predicted AV from ANN Model compared with the field (training).....	90
Figure 48 - Predicted AV from ANN Model compared with the field (testing).....	90
Figure 49 - Drilling parameters vs Depth – Showing hole cleaning conditions at depth of concern.....	92
Figure 50 - HCI model calculator showing good hole cleaning at depth 1908 ft.....	95
Figure 51 - HCI model calculator showing bad hole cleaning at depth 10692.8 ft .....	95
Figure 52 - HCI model calculator showing crucial hole cleaning (stuck pipe) at depth 12854.32 ft .....	96

## **LIST OF ABBREVIATIONS**

<b>ECD</b>	<b>:</b>	<b>Equivalent circulation density</b>
<b>TR</b>	<b>:</b>	<b>Transport Ratio ROP</b>
<b>RF</b>	<b>:</b>	<b>Rheology factor</b>
<b>AF</b>	<b>:</b>	<b>Angle factor</b>
<b>PV</b>	<b>:</b>	<b>Plastic viscosity</b>
<b>YP</b>	<b>:</b>	<b>Yield point</b>
<b>Cc</b>	<b>:</b>	<b>Cuttings concentration</b>
<b>v</b>	<b>:</b>	<b>Velocity</b>
<b>A</b>	<b>:</b>	<b>Area</b>
<b>HHP</b>	<b>:</b>	<b>Hydraulic horsepower</b>
<b>API</b>	<b>:</b>	<b>American Petroleum Institute</b>
<b>CCL</b>	<b>:</b>	<b>Carrying capacity index</b>
<b>JIF</b>	<b>:</b>	<b>Jet impact force</b>
<b>AI</b>	<b>:</b>	<b>Artificial Intelligence</b>
<b>AV</b>	<b>:</b>	<b>Annulus Velocity</b>
<b>CCI</b>	<b>:</b>	<b>Cutting Carrying Capacity</b>
<b>ECD</b>	<b>:</b>	<b>Equivalent Circulating Density</b>
<b>HCI</b>	<b>:</b>	<b>Hole Cleaning Index</b>
<b>HCR</b>	<b>:</b>	<b>Hole Cleaning Ratio</b>

|

## **ABSTRACT**

Full Name : [Mahmoud Nader Mahmoud Elzenary]

Thesis Title : [ESTIMATION OF HOLE CLEANING CONDITION IN REAL-TIME WHILE DRILLING (OPERATIONAL POINT OF VIEW)]

Major Field : [Drilling]

Date of Degree : [October, 2018]

Hole cleaning is the main parameter while considering the quality and efficiency of drilling deviated and horizontal wells. Hole cleaning is being affected with many factors while drilling such as: weight on bit (WOB), rate of penetration (ROP), rock geomechanics, drilling fluid properties, and rig hydraulics.

Hole Cleaning has a great impact on drilling efficiency, as the hole cleaning getting better the drilling overall efficiency will increase. Bad hole cleaning in many cases leads to non-productive time (NPT). Stuck pipe, slow ROP and drilling bit damage are common problems related to inefficient hole cleaning.

To measure the hole cleaning while drilling, field, and experimental measurements will need to be conducted with the complicated and high-cost process. For example, while drilling the rig crew will need to handle a long process of drilling parameter optimization (e.g. weight on bit, torque limit, flow rate, rate of penetration .... etc.) to achieve the best hole cleaning scenario for a specific section. This process will be costly as it will not be counted as productive time.

A lot of researches were conducted to evaluate the hole cleaning and related cutting transport efficiency while drilling. The main gaps in these researches come

from the fact that, these researches contain mainly experimental and empirical models which most of the time will not reflect all factors affecting the hole cleaning even it may also be not applicable in the field from the operational side of view.

With the new technology called Artificial Intelligence (AI) and its related applications such as; support vector machine (SVM), adaptive neuro-fuzzy interference system (ANFIS), and artificial neural network (ANN), downhole parameters affecting the hole cleaning process will be predicted with high accuracy and hence, with the right model the hole cleaning condition will be measured.

This thesis proposes new means of predicting hole cleaning in both vertical and highly deviated wells using a new model which includes two artificial intelligence models. The first artificial intelligence (AI) model was built to predict the drilling fluid rheology parameters (yield point YP and plastic viscosity PV). The second artificial intelligence (AI) model was built to predict the equivalent of circulation density (ECD) while drilling.

These two AI models will be part of a new approach called hole cleaning index (HCI) to estimate the hole cleaning condition in real-time bases while drilling in vertical to highly deviated wells with all ranges and through well different drilling sections.

|

## ملخص الرسالة

الاسم الكامل: محمود نادر محمود الزناري

عنوان الرسالة: تقدير نظافة البئر أثناء عملية الحفر (من وجهة نظر عملية)

التخصص: الحفر

تاريخ الدرجة العلمية: يناير ٢٠١٩

إن عملية نظافة البئر من أهم عمليات الحفر الحيوية التي يعتمد عليها مشغلي الآبار. إذا لم يكن البئر نظيفا من بقايا الحفر فإن مشاكل كثيرة سوف تحدث وتؤثر على عملية الحفر. من أخطر المشاكل المرتبطة بسوء حالة نظافة البئر هي إنحشار وإلتصاق عمود الحفر داخل البئر. الكثير من العوامل تؤثر على حالة نظافة البئر أثناء الحفر أهمها:

سرعة الحفر.

وخواص سائل الحفر.

للوصول لكفاءة عالية من عملية الحفر يجب متابعة عملية التنظيف بصورة دقيقة. سابقا كان يعتمد مشغلي الحفارات على خبرتهم و على متابعة بواقي الحفر عند هزاز الطمي ولكن ذلك لم يكن كافيا لتنظيف البئر بكفاءة مما يترتب عليه مشاكل جسيمة في عملية الحفر والتي تكلف شركات التنقيب الملايين من الدولارات.

مع ظهور التكنولوجيا المتقدمة مثل الذكاء الاصطناعي أمكن ذلك تطبيقه في عمليات كثيرة من عمليات التنقيب وإستخراج النفط. في هذا البحث سوف أستخدم الذكاء الاصطناعي في تقدير خواص سائل الحفر المؤثرة في عملية رفع بقايا الحفر من داخل البئر, أيضا سوف أستخدم هذه النتائج لبناء نموذج يستطيع أن يتعرف ويقدر حالة البئر أثناء الحفر, هل هو نظيف أم لا وهل هناك مشكلة في أسفل البئر تحدث أثناء الحفر أم لا.

مع وجود هذا النموذج ومع ربطه بنظام تشغيل الحفارة سوف يتمكن الحفار ومشغلي الآت الحفر من متابعة حالة أسفل البئر أثناء عملية الحفر وبهذا يمكنهم تحديد المشكلة قبل حدوثها داخل البئر, مما يساهم في تحسين كفاءة حفر القطاع بالصورة الأمثل. |





# CHAPTER 1

## INTRODUCTION

### 1.1 Background

The biggest challenge in drilling is to reach target depth (TD) without facing serious problems including: stuck pipe, formation break down and hole pack-off. All of these problems are directly linked to hole cleaning issues. To overcome the poor hole cleaning is the most effective way to achieve successful drilling operations.

Many factors are affecting the removal of drilled cuttings including the medium of transportation. One of the most critical functions of the drilling fluid is the ability to carry and suspend solids out of the hole. Carrying capacity of the drilling fluid is affected by several factors, including: rheology and density of the fluid, flow regime and annulus size, shape and size of cuttings, cuttings density and annulus size ([Tie Yan et al, 2014](#); [Ali Zakerian et al, 2018](#)).

Operative hole cleaning is of prodigious importance in oil well drilling operations, because insufficient hole cleaning can lead to, but not limited to the following severe problems: fill, packing off, stuck pipe and unnecessary hydrostatic pressure. Initially, it was considered that the primary purpose of the mud was to remove the cuttings continuously ([M. E. Hossain, M. R. Islam, 2018](#)).

Pipe eccentricity effect cannot be practically measured. One of the most important factors that affect the carrying capacity of mud is the velocity profile in the annulus. The velocity profile, in turn, depends on the annulus cross-sectional area, and the eccentricity of the inner core and its rotation. This work involves the use of Couette flow analysis to determine eccentricity, [Anon \(2010\)](#).

When the fluid is being confined between two cylinders (one stationary and the other is moving), this is known as Couette flow. The same phenomenon is occurring in the annulus, where the wellbore is the stationary cylinder and the drill pipe is the moving one. The fluid average velocity is a strong function of the velocity of the moving cylinder/pipe, [Chu Hyun, \(2000\)](#).

In deviated wells, the drill string lies along the low-side of the wellbore which will cause pipe eccentricity. Drill pipe eccentricity depends mainly on the hole depth and angle and will vary with different sections of the hole, [Jawad and Akgun \(2002\)](#).

Hole cleaning problems normally happen in deviated wells (**Figure 1**). The cuttings removal becomes more difficult when dealing with high deviated wells as the cuttings tend to lie on the wellbore low-side. Commonly more attention is required while drilling directional wells.

These problems include: stuck pipe, bit damage, slow rate of penetration, drilling losses, and excessive torque and drag.

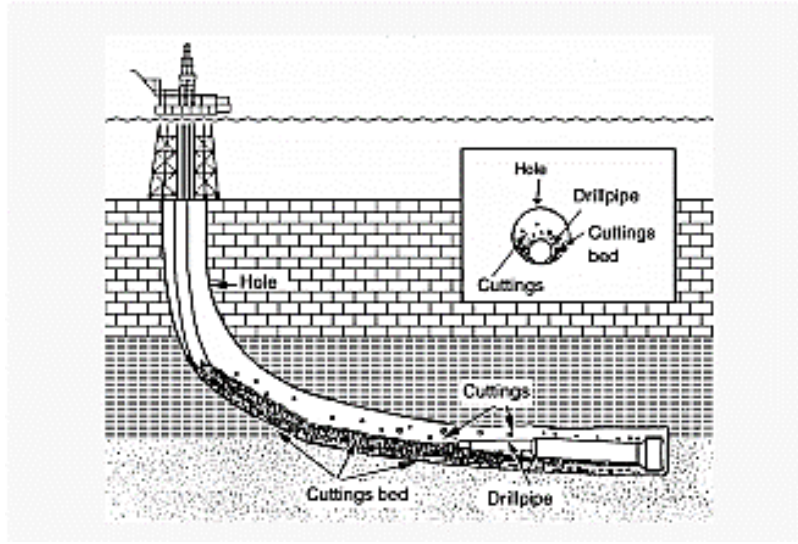


Figure 1 - Hole cleaning in deviated wells

Many parameters were developed to evaluate the hole cleaning condition with measurable functions as following:

Transport ratio (TR). 
$$TR\% = \left(1 - \frac{V_s}{V_l}\right) * 100 \quad (1.1)$$

$V_s$  is the particle slip velocity, and  $V_L$  is the fluid velocity in the annulus.

Hole Cleaning Ratio(HCR). 
$$HCR = \left(\frac{H_{cb}}{H_{cri}}\right) \quad (1.2)$$

$H_{cb}$  is the cutting bed height, and  $H_{cri}$  is the critical height of the cutting bed.

Transport Index (TI). 
$$TI = AF \times RF \times SG \quad (1.3)$$

**AF** is the Angle factor, **RF** is the Rheology factor, and **SG** is the specific gravity of the liquid.

Carrying Capacity Index(CCI). 
$$CCI = \left(\frac{Denisty(pcf)*K*V_{ann}}{7.491*400000}\right) \quad (1.4)$$

**K** is the consistency index for pseudoplastic fluid, and  $V_{ann}$  is the drilling fluid annulus velocity

Each one of these “hole cleaning indicators”, individually will not give the real hole cleaning condition happens downhole on real-time bases.

The objective of this dissertation is to; deeply understand the main parameters which affect the hole cleaning condition in real-time bases while drilling, build AI models that can be used to predict the downhole variables and parameters that directly affect the hole cleaning estimation and build an analytical model integrated with the AI models to develop a user-friendly software interface that will automatically predict the condition in real-time while drilling.

The way to an effective hole cleaning depends on coordinating ideal drilling fluid properties with best drilling practices. In the field, diagrams have been produced which can be utilized to predict. hole cleaning in wells with deviation greater than 25 degrees, previously, hole cleaning in vertical and near vertical wells have been predicted by calculating the carrying capacity index (CCI), ([www.ballots.api.org](http://www.ballots.api.org)).

## **1.2 Significance, Scope and Definitions**

Viscosity, well-defined as the relation between shear stress and shear rate, the viscosity for most drilling fluids is not constant but varies with the shear rate. So, we use the term effective viscosity to show that it was measured at a specific shear rate at existing flow conditions in the wellbore.

Shear stress is the force needed to sustain a particular fluid flow rate, it is the ratio of force to the given area. Shear rate, this is the fraction between the velocity to the distance (velocity gradient), it can be perceived as the frequency at which one layer of fluid is stirring past

another layer. Shear rate is not constant across the flow channel and is highest next to the pipe wall, [www.era.library.ualberta.org](http://www.era.library.ualberta.org).

A vertical well is any well with an inclination of 0 degrees, but most oil wells are drilled at an angle. So, for the purpose of this work, we shall define a vertical well as one with an angle of less than 5 degrees.

Mud weight, also known as the fluid density, is the mass per unit volume of the fluid. It is a very important property of the drilling fluid. Newtonian fluid is any fluid that exhibits the following behaviors: (a) The only stress generated in simple shear flow is the shear stress, the two-normal stress difference being zero, (b) shear viscosity does not vary with shear rate, (c) viscosity is constant. A non-newtonian fluid is any fluid showing deviation from Newtonian behavior, most drilling fluids fall into this group, i.e. viscosity varies with shear rate, [Owens \(2002\)](#).

Critical velocity is the velocity at which cutting transport is optimized, where the Reynolds equal the critical Reynolds number. The Critical flow rate is the flow rate at which the rate equals the critical velocity. During fluid flow, the flow patterns and friction factors can be considered as laminar, transitional and turbulent flow regimes. A term introduced when more than one phase is flowing downhole, i.e. slip velocity: the difference between the gas and liquid velocity. |

## CHAPTER 2

### LITERATURE REVIEW

Ideal hole cleaning refers to the efficient elimination of drilling cuttings, for this condition to hold, many factors must be in place. To efficiently transport cuttings out of the hole, the transporting medium (drilling fluid) must be able to suspend the solid particles; also, there must be enough energy in the form of a motion to push the solids out of the hole. Many researchers have been conducted to identify some of the factors affecting hole cleaning.

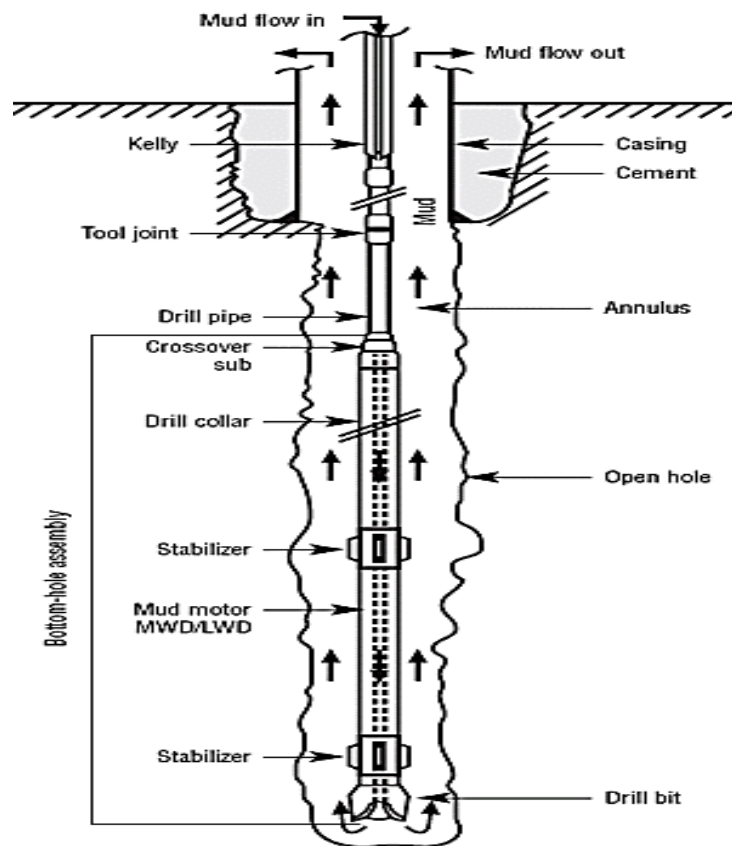


Figure 2 - Drilling Fluid movement downhole

The basic medium for cutting transport during drilling is via the circulation fluid better known as the drilling fluid. Cutting suspension and transport is one of the most important properties to be considered when selecting the drilling fluid, [E. Ghasemi et al, \(2016\)](#). **(Figure 2)** is showing the movement of the drilling fluid in a vertical well is depicted below:

## 2.1 Factors Affecting Hole Cleaning

There are numerous factors that affect the capability of the drilling fluid to capably transport cuttings to the surface and afford ideal hole cleaning, some of such factors include: cutting size, drill pipe eccentricity, cutting density and mud weight, hole size and hole angle, rheology of circulation fluid, drill pipe rotation, multi-phase flow effect, hole cleaning pills, rate of penetration (ROP), cuttings transport ratio, and cuttings bed properties. [Tie Yan, et al \(2014\)](#).

[Rishi et al \(2000\)](#) had developed a method to determine the optimum mud properties and drilling fluid flow rates to increase the hole cleaning efficiency in decidedly deviated and horizontal wells. In this study, a new empirical model was developed to integrate the mud properties and the pump rate to the hole cleaning process. **Figure 3** summarized the factors affecting the cutting transport efficiency within the field.

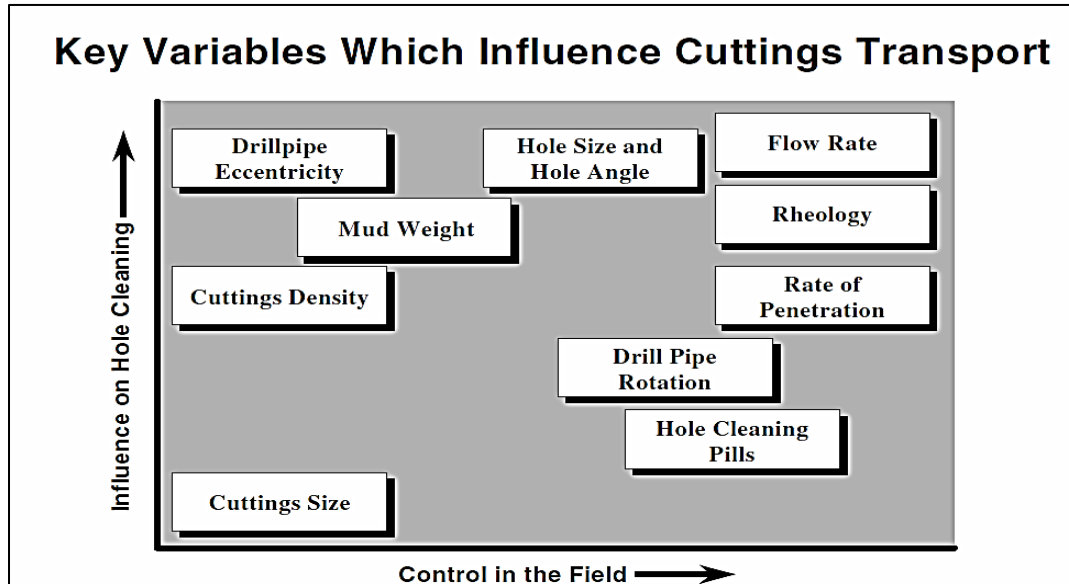


Figure 3 - Key variables controlling cuttings transport

Significant enhancement in the cutting transport efficiency in the hole was achieved through this study when  $n/k$  ratio –  $n/k$  ratio define the flow regime – increased (turbulent flow). Turbulent flow regime had improved the cuttings removal process. As the hole angle increased a significant increase in the circulation time required to clean the well. The authors did not include the effect of pipe rotation speed with the cuttings transport process.

### 2.1.1 Cutting/Particle Size

Cutting characteristics such as density, size and shape are connected to their behavior in a flowing media. Properties of the circulation fluid with its fundamental properties have an effect on the cuttings between the average velocity, slip velocity, buoyant forces and shear forces. The sphericity of the cutting particle is the proportion of the surface area of a sphere of the same volume to the surface area of the particle.



$$S p h e r i c i t y = \frac{A_s(s p h e r e)}{A_s(p a r t i c l e)}$$

(2.1)

The table below shows the sphericity for cutting particles of different shapes, [www.pnnl.gov](http://www.pnnl.gov)

**Table 1 - Sphericity for different cuttings shapes**

Shape	Sphericity
Sphere	1.0
Octahedron	0.85
Cube	0.81
Prism	0.77

According to the investigation, there is a particle magnitude that stances the most struggle to clean out with water and from their research; it is of the order of 0.76 mm diameter. They also concluded that smaller particles are harder to be removed if compared to larger ones when the particle size is larger than 0.5 mm, but for particles smaller than 0.5 mm, the minor particles are easier to be cleaned out. Another factor which affects the critical velocity needed to transport dissimilar sizes of particles is cutting concentration, [S. Walker, \(2000\)](#).

### **2.1.2 Drill Pipe Eccentricity**

In vertical wells, it is easier to achieve a well-centered drill string, but in deviated and high angle well, the drill string continuously inclines to lie on the hole low side due to gravity. Experiments by [Walker, S and J. Li \(2000\)](#) showed that solids are more difficult to be transported when the pipe is situated near the bottommost side of the hole. When this happens, the velocities in the fine gaps near to the pipe are very low and this will cause solids to be dropped quickly. This

consequence tends to be highlighted if the viscosity increases, as the drag forces on the liquid will reduce the velocity in the narrow gap the more.

An industrial method to estimate eccentricity is a function of concentric-annulus pressure loss in each segment by the empirically derived ratio  $R_{lam}$  or  $R_{turb}$  depending on the flow regime:

$$R_{lam} = 1,0 - 0,072 \frac{e}{n} \left[ \frac{d_p}{d_h} \right]^{0.8454} - \frac{3}{2} e^{2\sqrt{n}} \left[ \frac{d_p}{d_h} \right]^{0.1852} + 0,96 e^{3\sqrt{n}} \left[ \frac{d_p}{d_h} \right]^{0.2527} \quad (2.2)$$

Where:

$R_{lam}$	Eccentric annulus laminar pressure ratio (dimensionless)
$e$	Eccentricity
$n$	Flow behavior index (Herschel-Bulkley fluids)
$D_p$	Pipe outside diameter
$D_h$	Hole diameter or casing inside diameter

This equation is used to calculate the eccentricity of the drill pipe in laminar flow. For calculation during turbulent flow conditions, we use the following:

$$R_{turb} = 1,0 - 0,048 \frac{e}{n} \left[ \frac{d_p}{d_h} \right]^{0.8454} - \frac{2}{3} e^{2\sqrt{n}} \left[ \frac{d_p}{d_h} \right]^{0.1852} + 0,285 e^{3\sqrt{n}} \left[ \frac{d_p}{d_h} \right]^{0.2527} \quad (2.3)$$

Where:

$R_{turb}$	Eccentric annulus turbulent pressure ratio
$e$	Eccentricity
$n$	Flow behavior index (Herschel-Bulkley fluids)
$D_p$	Pipe outside diameter
$D_h$	Hole diameter or casing inside diameter

(Figure 4) shows the effects of pipe eccentricity on fluid movement are shown. Cutting transport is most efficient in zone B where the pipe is well centered, while such is not the case in zones A and C where the pipe lays on one side.

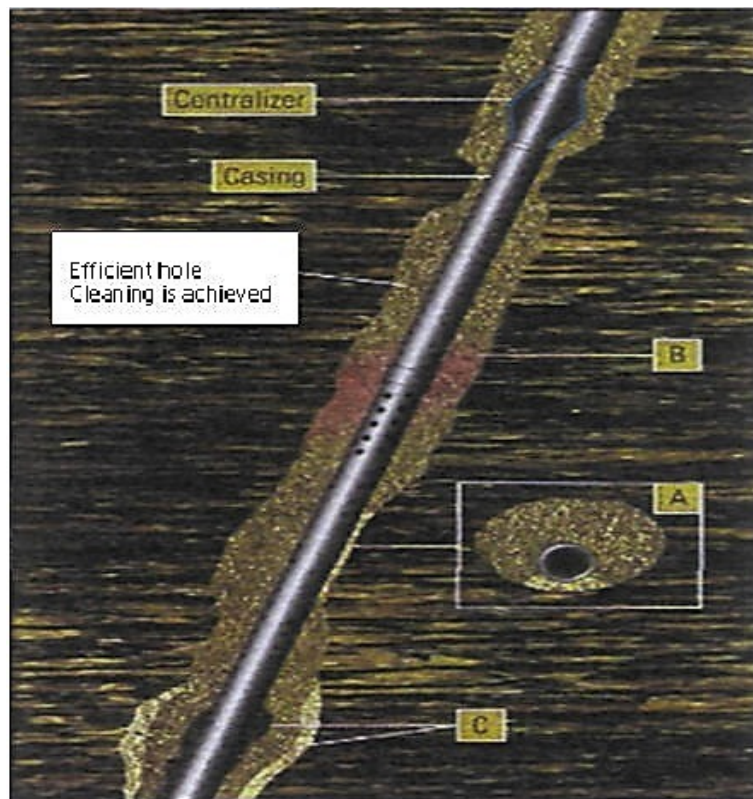


Figure 4 - Depiction of pipe Eccentricity

It is important to note that cutting removal is affected slightly by the pipe position in the hole at a low angle. As the inclination of the well increases towards the horizontal, the amount of

fluid needed for proper hole cleaning increases. In conclusion, hole cleaning time is affected by the pipe position within the wellbore. For hole cleaning optimization, reliable method for pipe eccentricity prediction is needed.

### 2.1.3 Drill Pipe Rotation

It has been suggested that cutting transport is made easier in the presence of drill pipe rotation, (Figure 5), [N. Moroni, \(2009\)](#). Semi-consolidated beds can in some cases be removed because the drill string drags a large portion of the bed around from the bottom of the annulus to the top where a high flow rate. The high flow rate can then disperse the removed cuttings to some degree and good hole cleaning might be accomplished. This behavior is especially a plausibility for removing sand beds and other non-reactive cutting particles, [A. Saasen \(2002\)](#).



Figure 5 - Pipe rotation helps fluid flow in the narrow side of an eccentric annulus

Because of drill pipe rotation, fluid flow among the formation and a rotating pipe or a cased well are rarely stable. Pipe rotation tends to make flow turbulent and this turbulent similar

to motion makes the frictional pressure loss to rise, causing an increased shear stress on the cutting bed surface. This enlarged shear stress will back the cutting removal process. Pipe eccentricity is hardly achieved in most wells, in eccentric cases the pressure loss and thereby the ability to remove cuttings is increased because the effect of pipe rotation causes debauched flowing fluid from the wide portion of the hole down into slender sections inserted between the formation and the drill pipe.

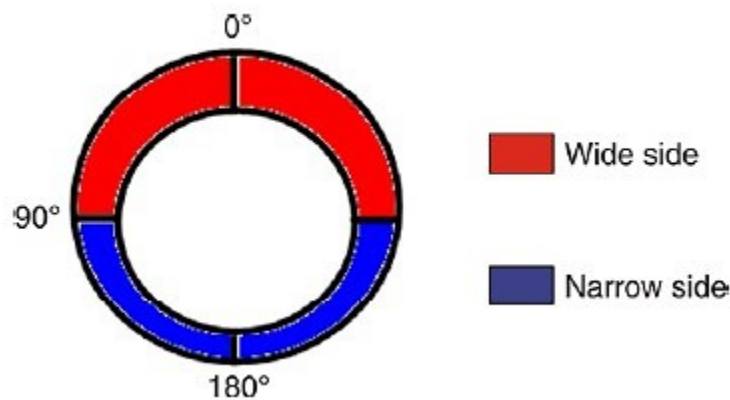


Figure 6 - Illustration of wide and narrow sides in an eccentric annulus

The fluids originally flowing through the narrow side is forced to move to the wide areas where the fluid velocity is higher, (**Figure 6**). So, the fluid in the narrow side is forced to accelerate. This alternating acceleration and retardation create an increase in annular pressure losses. The bigger the rotation rate, the extra turbulence like the motion becomes and the frictional pressure losses growths. Therefore, for optimal hole cleaning, it is recommended to use as high drill pipe rotation as conceivable.

Ayad A. Al-Razzaq et al, (2016) had discussed the effect of the drill string rotation, he proved that it has a significant effect on the hole cleaning and cutting removal process while drilling. He showed that in the presence of high viscosity mud the effect of drill pipe rotation on

hole cleaning enhancement became greater. He proved that for hole inclination at 65 degrees, and at horizontal, the effect drill string rotation created an enhancement in cuttings removal as shown in (Figure 7 and Figure 8), [Kien Lim, \(1996\)](#); [Heshamzadeh, \(2016\)](#).

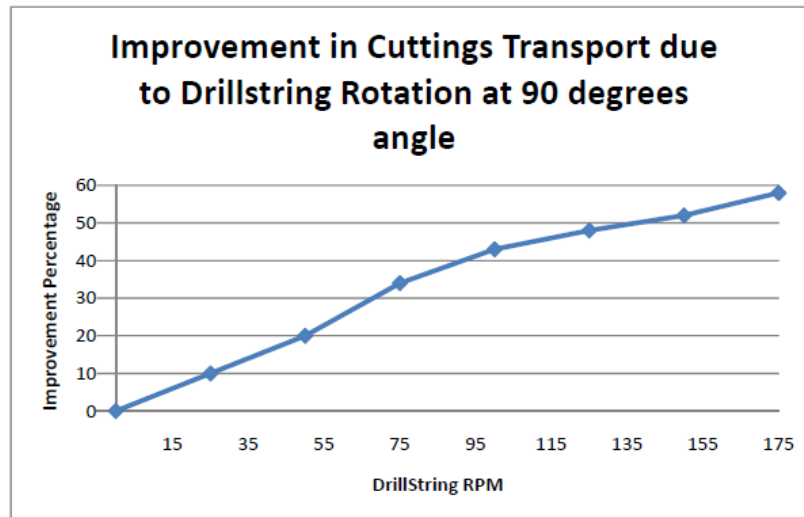


Figure 7 - Effect of drill string rotation on cuttings transport in a horizontal wellbore

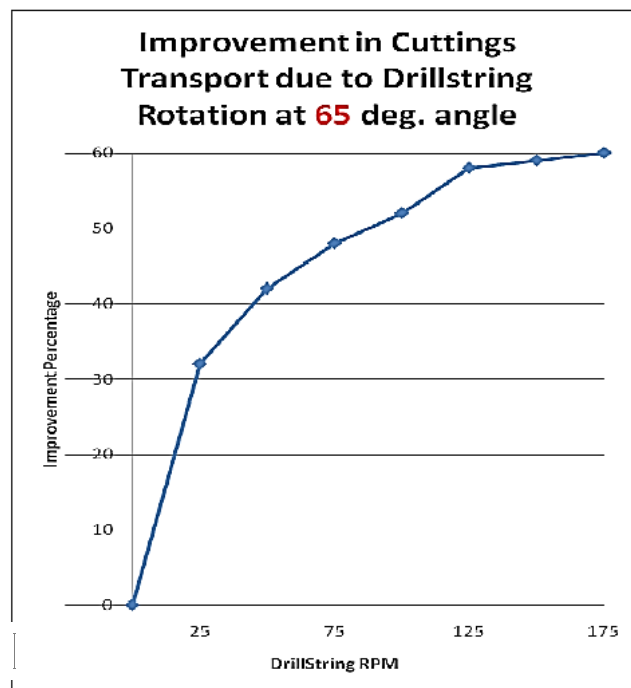


Figure 8 - Effect of drill string rotation on cuttings transport in a wellbore at 65 degrees angle

Once the pipe is not rotated, there is no fluid in the circumferential path. Owing to the fundamental difference in the shear geometry between the narrow and wide sides of the annulus, the difference in the top of the fluids is caused because of that the flow rates in the narrow side are always lower than those in the wide side. When the pipe is rotated, tangential velocity in the fluid begins across the annulus gap, starting next to the casing. This leads to the transfer of fluid from the wide side to the narrow side, and vice versa, [N. Moroni, \(2009\)](#).

It should be noted that drill pipe rotation will affect the cuttings bed fraction differently depending on cutting bed rheology. For a bed formed in an oil-based drilling fluid, there should be no gel structure that connects the cutting particles. Meaning that drill pipe rotation would primarily transport only the bed's surface particle into the annulus mainstream flow, but a water-based drilling fluid with many polymers can compose a gel structure inter-linking the different cutting particles in the bed. Drill pipe in this condition can transmit a larger volume of cutting to the annular mainstream. As the polymer content of the water-based drilling fluid decreases, the influence of the drill pipe rotation on the cutting bed decreases, [A. Saasen \(1998\)](#).

#### **2.1.4 Hole Size and Hole Angle**

Studies have established the importance of the effect of the inclination angle in cutting transport. [J. Li and S. Walker \(1999\)](#) showed that the toughest section for hole cleaning is the build section rather than the vertical or the horizontal section (**Figure 9**).

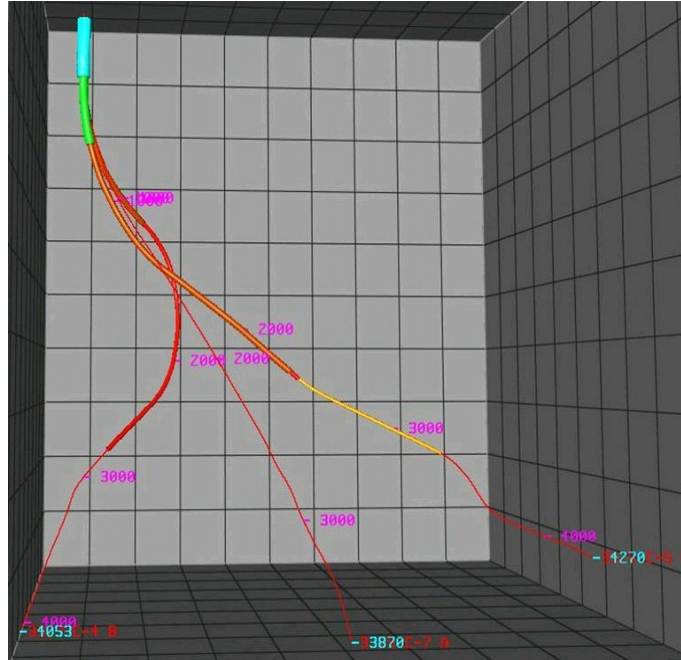


Figure 9 - Effect of hole angle on particle sedimentation

In vertical wells with inclination less than 20 degree, the particles settle within the fluid, and the settling rates are generally low. In Deviated wells with inclination between 20 degree, and 70 degree the particles settle out of the fluid, contact the borehole wall and slide downwards (Boycott settling). In horizontal wells with inclination greater than 70 degree the particles settle out of the fluid but do not move after this.

As the inclination angle varies, the liquid velocity varies. The highest minimum in-situ liquid velocity is needed around 60 degrees as shown in (**Figure 10**). This is because cuttings tend to become unstable and to slide downward along the wellbore when angle increases above 60 degrees. Thus, hole cleaning is most difficult at close to 60 degrees, [J. Li and S. Walker \(1999\)](#); [Jeff Li, \(2001\)](#).



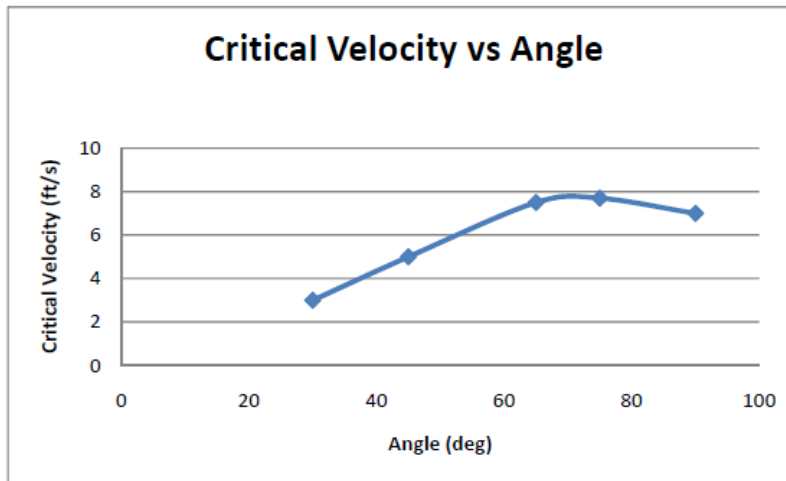


Figure 10 - Effect of inclination angle on the critical velocity

### 2.1.5 Rheology

Rheology can be defined as the science of deformation and flow, it refers to the extraordinary and characteristics of the drilling fluid. These properties of the circulation fluid have an effect on solids transport, [www.benthamopen.com](http://www.benthamopen.com).

Monitoring the drilling fluid rheological properties is one of the most effective tools to prevent drilling operations downhole problems. Apparent viscosity, plastic viscosity, and yield point are the most important parameters to ensure hole cleaning efficiency while drilling the well. In the field, only Marsh funnel viscosity is measured every 10 mins. Plastic viscosity and yield point are measured frequently twice or once a day, [Seyed et al, (2018); Yun-Kui Yan (2007)].

There are three main types of drilling fluid based on the base fluid. Oil base mud, water base mud and gas base mud, Caenn et al., (2011). Oil based mud (OBM) contains oil as the continuous phase and water as the dispersed one (less than 5% water ratio). OBM is being used in the drilling industry for certain formations which can react with the water based mud (WBM)

if being used instead. OBM mainly consists of density weighting material, emulsifier and filtration control material. OBM is commonly used at high-temperature conditions due to its high stability compared to WBM under the same conditions ([Bourgoyne et al., 1991](#); [Abdo and Haneef, 2012](#); [Salaheldin et al., 2016](#)).

When OBM contains 50% as water ration, it is called invert emulsion mud. It has an advantage being low toxicity mud with oil as the continuous phase and water with Calcium Chloride ( $\text{CaCl}_2$ ) is the dispersed phase. The presence of  $\text{CaCl}_2$  increases the salinity and that decreases the reaction of water with the formation, [Hossain, and Al-Majed \(2015\)](#).

To monitor mud rheological properties, laboratory instruments will be used. Mainly mud balance, API filter press, and viscometer are being used daily in the mud lab. To have accurate measurements for the mud rheological properties, long time will be wasted on these lab measurements. Common mud properties for drilling a well; mud density (formation pressure control), plastic viscosity and yield point (hole cleaning).

Rig site considerations are important while dealing with drilling fluid properties. A complete mud test is done once in the morning and once in the evening. Marsh funnel is being used to measure the mud viscosity every 15 mins. [Marsh \(1931\)](#), has provided his funnel with specific dimensions which give accurate viscosity indication when being used to fill a cup of 930  $\text{cm}^3$ .

Diverse models have been spread to provide help with portraying fluid flow, however, none of these models can totally describe rheological properties of drilling fluids over their whole properties. ([www.sciencepublishinggroup.com](http://www.sciencepublishinggroup.com)), the Bingham Plastic Model is used in

fluids in which the shear stress to shear rate ratio is linear when a specific stress is exceeded.

Mathematically, it is given as:

$$\sigma = \sigma_y + \eta_p \gamma \quad (2.4)$$

Where:

$\sigma$	Shear stress
$\eta_p$	Flow behavior index (power law fluids)
$\gamma$	Shear rate ( $s^{-1}$ )

For such fluids, a specific yield stress must be exceeded for the fluid to flow. The model uses  $\theta_{300}$  and  $\theta_{600}$  to calculate the basic parameters PV and yield point YP.

$$PV = \theta_{600} - \theta_{300} \text{ (PV in cP)} \quad (2.5)$$

$$YP = \theta_{300} - PV \text{ (YP in } \frac{lb_f}{100ft^2}) \quad (2.6)$$

Where:

$\theta_{300}$	Viscosity reading at 300 Rpm (cP)
$\theta_{600}$	Viscosity reading at 600 Rpm (cP)

Also, the Herschel-Buckley Model, also known as the modified power law model is used to describe the flow of pseudo-plastic drilling fluids which require a yield stress to flow. It is given mathematically as:

$$\tau = \tau_y + k \gamma^n \quad (2.7)$$

Where:

$\tau_y$	Suspension parameter
K	Consistency parameter
n	Flow behavior index
$\gamma$	Shear rate ( $s^{-1}$ )

In the Herschel-Buckley model, the consistency parameter k can be considered as the PV or plastic viscosity term in the Bingham plastic model, also, the  $\tau_y$  parameter is describing the suspension characteristics of a drilling fluid can be seen as the Bingham plastic model Yield Point, [Seyed et al., \(2018\)](#).

$$\tau_y = 2\theta_{300} - \theta_{600} \quad (2.8)$$

The fluid flow index is calculated using

$$n = 3.32 \log_{10} \left[ \frac{\theta_{600} - \tau_y}{\theta_{300} - \tau_y} \right] \quad (2.9)$$

Then the consistency index is gotten via:

$$k = \frac{(\theta_{300} - \tau_y)}{511^n} \quad (2.10)$$

Finally, the Power Law model, which is used to describe the flow of shear thinning or pseudo-plastic drilling fluid. A true power law does not exhibit a yield stress. This model uses two sets of viscometer dial readings to calculate index n and consistency index k for pipe flow and annular flow.

For pipe flow:

$$n_p = 3.32 \log_{10} \left[ \frac{\theta_{600}}{\theta_{300}} \right] \quad (2.11)$$

$$k_p = \frac{\theta_{300}}{511^{n_p}} \quad (2.12)$$

Where:

$K_p$	Consistency factor(power law)
$n_p$	Flow behavior index (power law fluids)

While for annular flow :

$$n_a = 0.657 \log_{10} \left[ \frac{\theta_{100}}{\theta_{300}} \right] \quad (2.13)$$

$$k_a = \frac{\theta_{100}}{170.3^{n_a}} \quad (2.14)$$

Where:

$n_a$	Annular flow behavior index
$K_a$	Annular consistency parameter

The methods and formulas for determining basic variables using different Rheology models are summarized in the **tables 2 and 3**:

Table 2 - Equations for determining flow behavior parameters

<i>Rheological Model</i>	<i>Flow Behavior Parameter</i>
Newtonian	$\mu = \theta_{300}$
Bingham Plastic	$\mu_p = \theta_{600} - \theta_{300}; \tau_y = \theta_{300} - \mu_p$
Power Law	$n = 3.32 \log \frac{\theta_{600}}{\theta_{300}}; k = \frac{510 \theta_{300}}{511^n}$

Where:

$\mu$	Viscosity (cP)
$\mu_p$	Plastic viscosity (cP)
N	Flow behavior index (Herschel-Bulkley fluids)
$\theta_{300}$	Viscosity reading at 300 Rpm (cP)
$\theta_{600}$	Viscosity reading at 600 Rpm (cP)
$\tau_y$	Suspension parameter
K	Consistency parameter

Table 3 - Equations for determining average velocity

<i>Rheological Model</i>	<i>Average Velocity</i>	<i>Average Velocity in Annulus</i>
Newtonian, Bingham Plastic, Power Law	$\bar{v} = \frac{q}{2.448 d^2}$	$\bar{v} = \frac{q}{2.448(d_2^2 - d_1^2)}$

Where:

$\bar{V}$	Average velocity (cP)
q	Flow rate ( ft <sup>3</sup> / min )
d <sub>1</sub>	Inner diameter (ft)

The rheological properties of the mud will go a long way in determining its flow rate and suspension characteristics. According to [Zhang, Feifi. \(2015\)](#) – (**Figure 11**) - as the flow rate increases, the amount of cuttings in the annulus will decrease as shown below.

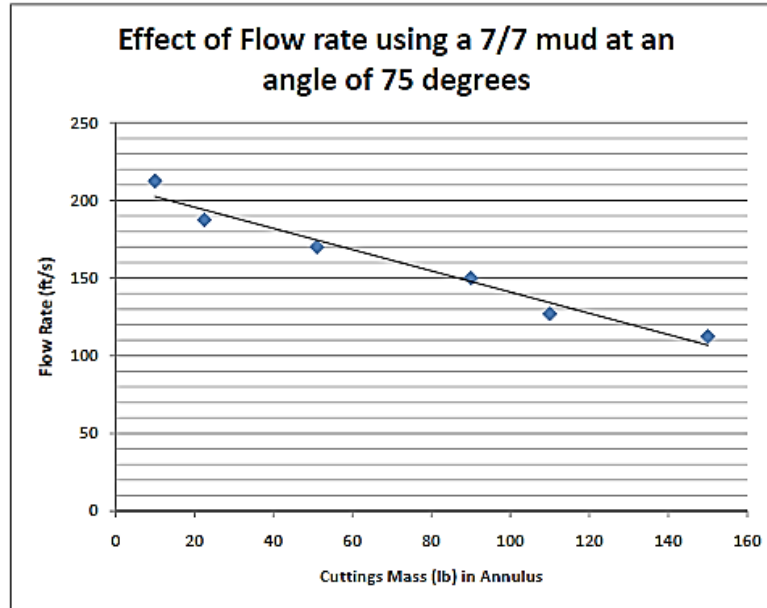


Figure 11 - Effect of mud flow rate on annular cuttings mass concentration

## 2.1.6 Cutting Transport Ratio

This is the proportion of the cuttings concentration that is conveyed or expelled from the hole to the aggregate cutting concentration in the wellbore annular space. When a relatively lesser amount of solids stays in the wellbore and a greater amount is transported with the carrying fluid, this is called a higher cutting transport ratio. So, cutting transport proportion ( $T_r$ ) can be viewed as the transport velocity ( $V_t$ ), divided by the fluid average annular velocity, [M.N. Belavadi \(1994\)](#). ( $V_f$ ) and is given by the equation:

$$T_r = \frac{V_t}{V_f} \quad (2.15)$$

Where the transport velocity is obtained using the following equation;

$$V_t = \frac{L}{t} \quad (2.16)$$

Where the length (distance), L, and time, t, are measured experimental data. The higher the transport ratio, the better the hole cleaning.

Researches have revealed that a critical flow rate exists at which cutting transport is optimized, and the well is efficiently cleaned. This critical flow velocity or flow rate have been modeled using different rheological models.

Using the power law model for fluids, we have:

$$V_{cp} = \left[ \frac{28277 (2.533 - n_p) k_p}{P} \left( \frac{1.6 G_p}{d_{hyd}} \right)^{n_p} \right]^{\frac{1}{2 - n_p}} \quad (2.17)$$

Where:

$$G_p = \left[ \frac{(3 - \alpha) n_p + 1}{(4 - \alpha) n_p} \right] \left[ 1 + \frac{\alpha}{2} \right] \quad (2.18)$$

Where:

$G_p$	Geometric shear-rate correction
$\alpha$	Angle between center point
$d_{hyd}$	Hydraulic diameter
$n_p$	Flow behavior index (power law fluids)

Using the Bingham-plastic model, we have:



$$V_{cb} = \frac{67.86}{\rho} \left[ B + \sqrt{B^2 + 9.42 \rho YP \left( \frac{4-\alpha}{3-\alpha} \right)} \right] \quad (2.19)$$

Where:

$$B = \frac{PV \left( 1 + \frac{\alpha}{2} \right)}{d_{hyd}} \quad (2.20)$$

Where:

B	Expansibility of conduit
V <sub>cb</sub>	Critical velocity (Bingham Plastic Fluid)
ρ	Density (lb/gal)
PV	Plastic viscosity (cP)

A very close approximation can be achieved by an empirical combination of the critical velocity based on Power-law and that based on Bingham-plastic model. Using these we have:

$$V_c = V_{cp} + (V_{cb} - V_{cp}) R^{\sqrt{\frac{V_{cp}}{V_{cb}}}} \quad (2.21)$$

Where:

$$R = \frac{\tau_y}{YP} \quad (2.22)$$

Where:

$V_c$	Critical velocity
$V_{cb}$	Critical velocity (Bingham Plastic Fluid)
$V_{cp}$	Critical velocity (power-law)
$R$	Wellbore radius
$\tau_y$	Suspension parameter
YP	Yield point (lb/100 ft <sup>2</sup> )

### 2.1.7 Rate of Penetration

According to studies by [J. Li (2001); J. Li (1999)], the cutting bed is more profound for a higher ROP than it is for a lower ROP with the same circulation fluid rate. Likewise, lower bed height results for a given ROP higher circulation fluid flow rate. Increasing the circulation flow rate results in lower cutting concentration and a decreasing of the bed height when the ROP is constant. Additionally, increasing ROP results in a higher cutting concentration and a higher bed height, with a fixed circulation rate.

According to Larsen, T.I.F (1990), the critical velocity increases with an increase in the rate of penetration (**Figure 12**). For an 8-inch hole size, with a 4-inch pipe diameter and an eccentricity of 62% at an angle of 45 degrees, he got the following graph for a 25/25 mud.

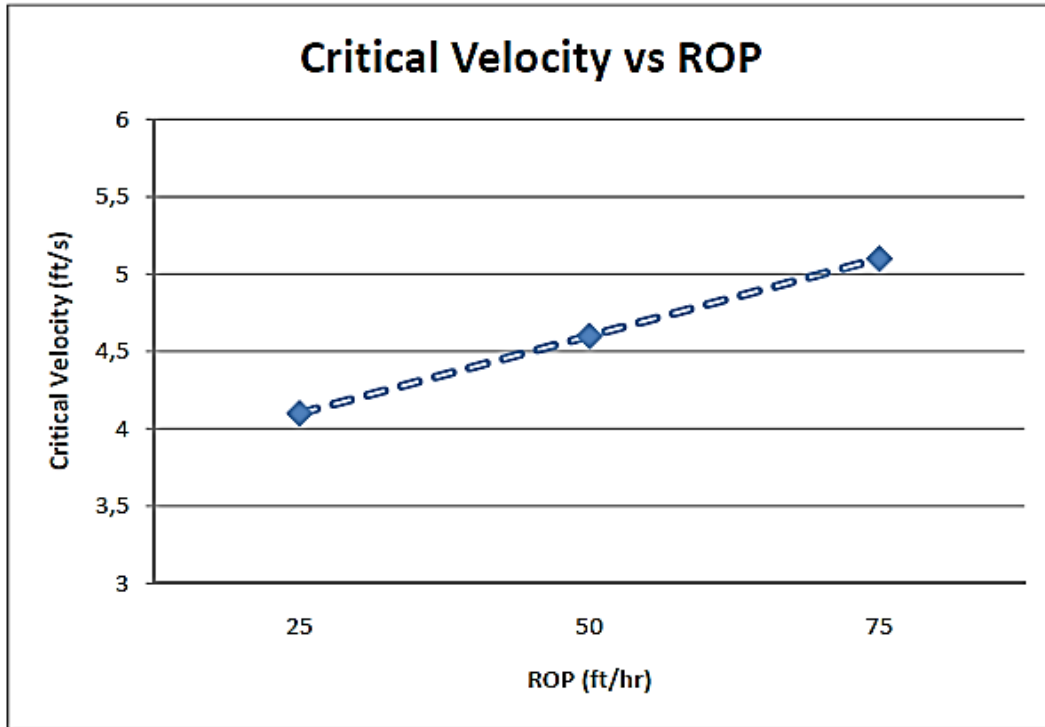


Figure 12 - Effect of ROP on the critical velocity

The cuttings velocity is a function of the rate of penetration as given in the equation below, E. Kuru (2004).

$$V_{cut} = \frac{ROP}{36 \left[ 1 - \left( \frac{D_{pipe}}{D_{hole}} \right)^2 \right] C_{conc}} \quad (2.23)$$

Where according to Rudi:

$$C_{conc} = 0.01778 ROP + 0.505 \quad (2.24)$$

## 2.2 FLOW PATTERNS AND FORCES ACTING ON DRILL CUTTINGS

### 2.2.1 Flow Patterns

Liabale on the flow rate, conduit shape, fluid and solid properties and inclination, the liquid and solid stages may dispense in a number of different geometrical configurations during the flow of solid-liquid mixtures as is obtainable during drilling operations. It is possible to have a fully suspended symmetric flow pattern, asymmetric flow pattern or a moving bed flow pattern, [V. C. Kelessidis, \(2003\)](#).

Completely suspended symmetric flow pattern is found when the liquid velocity is very high, such that the solids are uniformly distributed in the liquid phase; it is most observed when the solid particles are fairly fine-less than 1mm. As the liquid flow rate is reduced, there is a propensity for the solids to flow near the bottom of the pipe in highly inclined wells but still postponed, creating an asymmetric solid concentration. This is known as asymmetric flow pattern. If the flow rate is further reduced, solids might deposit on the low side and bottom of the pipe in horizontal and highly inclined wells, forming a bed which will move in the direction of flow: this is the moving bed flow pattern [V. C. Kelessidis, \(2003\)](#)..

When velocity is further reduced, there will be more deposition of solids, resulting in three layers, the top most consisting of a heterogeneous liquid, a moving solid bed and a stationary solid bed at the bottom. The diagram below depicts the different flow patterns (**Figure 13**), [Cho Hyun, \(2000\)](#).

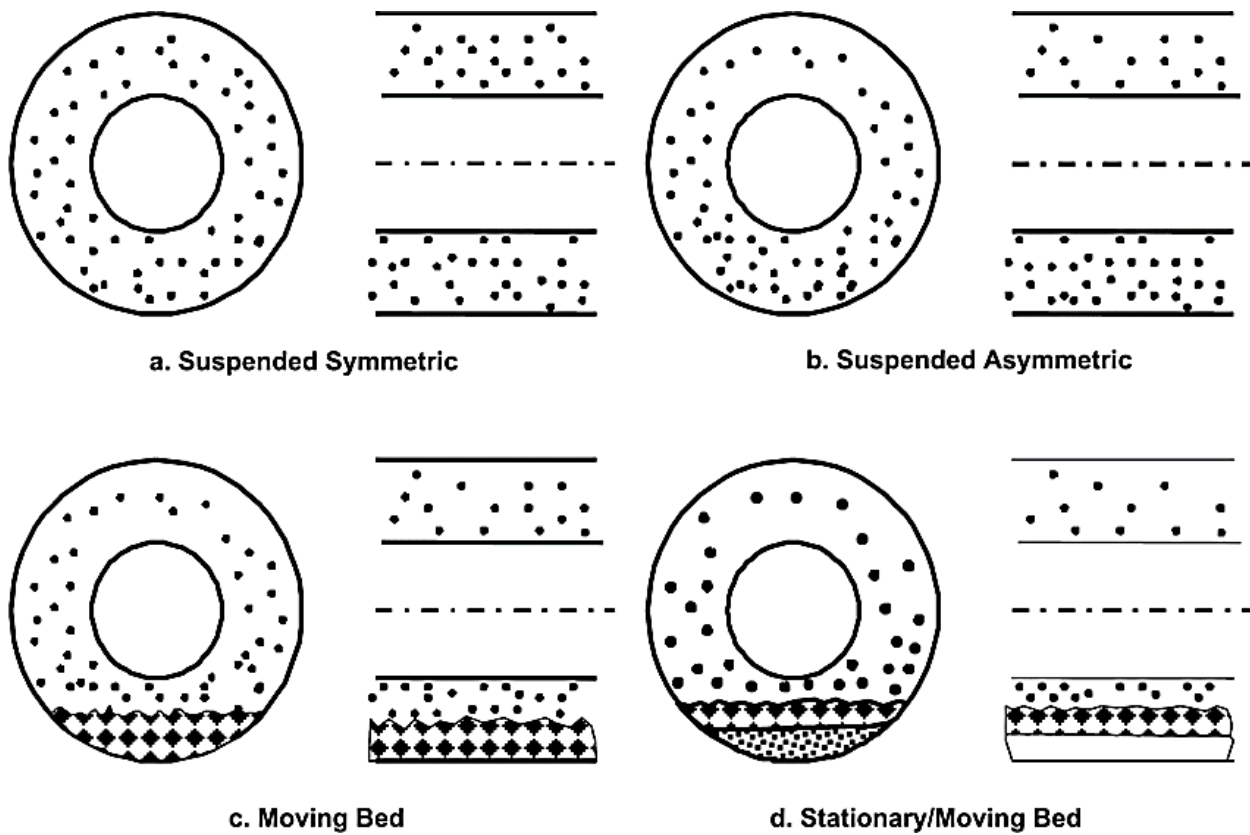


Figure 13 - Flow patterns for solids/liquid flow in high angle and horizontal annulus

### 2.2.2 Forces Acting on a Suspended Drill Cutting

A drill cutting in suspension is acted upon by different forces; it is also affected by the effect of other drill cutting in contact with it. The shape of the cutting and the fluid properties are very important in determining which force is most active and dominates the system, [Mingqin Duan, \(2007\)](#). The diagram below shows the fluid movement about a suspended and settling particle (**Figure 14**).

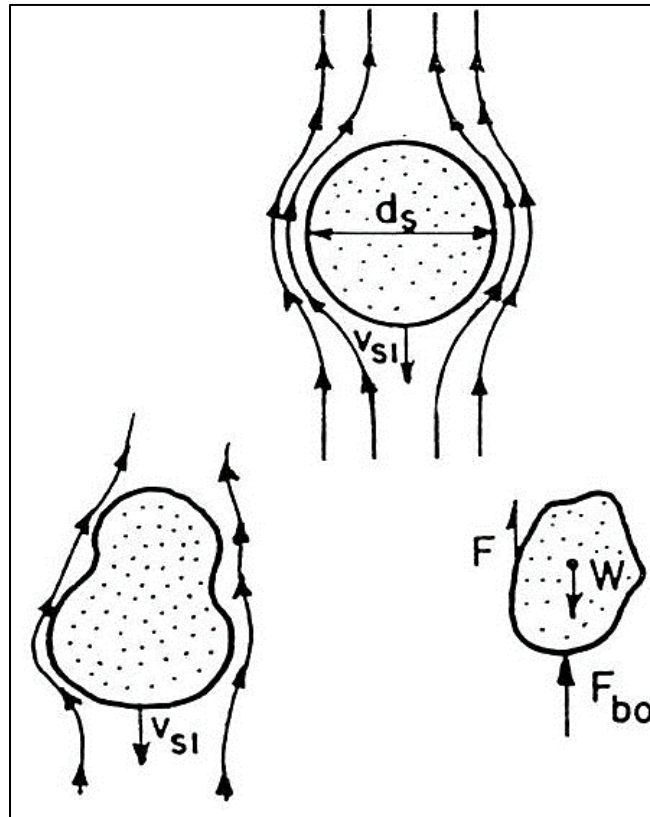


Figure 14 - Streamline of fluid movement about a settling or suspended particle

For a particle in suspension, the major forces acting on it includes the lift and drag forces, gravity and buoyancy forces, normal forces at the point of contact and frictional forces. These forces can be grouped into three groups. the stationary forces, hydrodynamic forces and the interparticle forces. Gravity and buoyancy forces are static forces due to the assets of the elements and its surrounding fluid. Drag and lift are hydrodynamic forces incurred from the fluid flow (**Figure 15**). Van der Waals forces are inter-particle forces existing between any neighboring particles. They become dominant when the diameter of two closely neighbored particles is below 0.1mm.

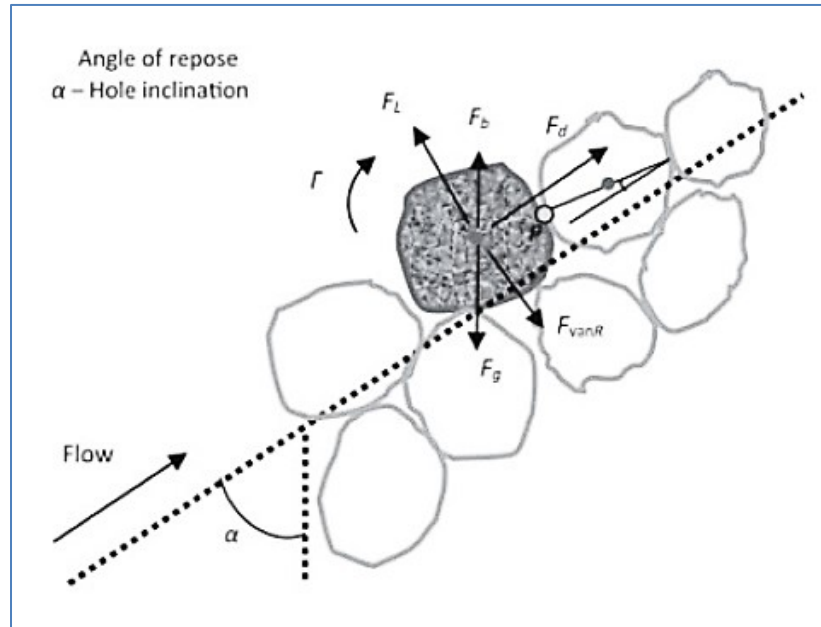


Figure 15 - Forces applied to a particle on a solids bed

Assuming the flow is stable and isothermal in a concentric annulus, the gas phase is free of cuttings, only spherical and uniform particles, no effect for the rotation of the inner pipe and cutting bed surface is uniform along the annulus (**Figure 16**), [Lei Zhou, \(2006\)](#) predicted:

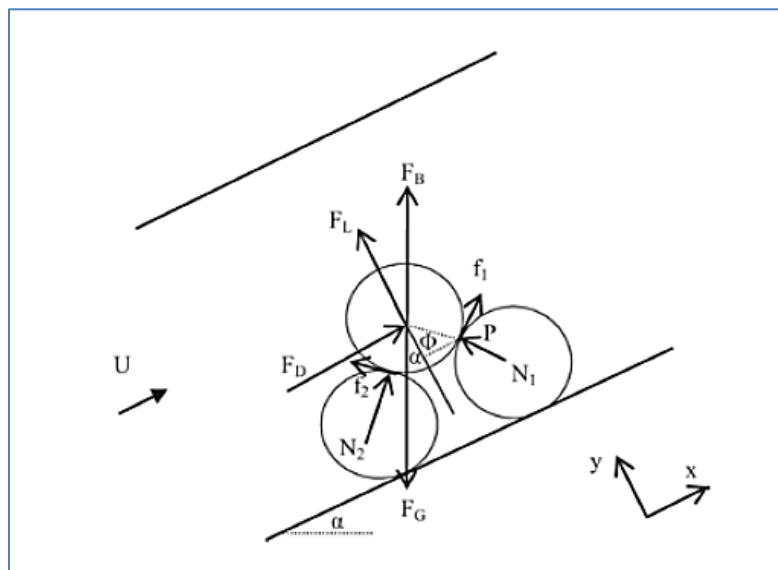


Figure 16 - Forces acting on a single particle

Static Forces, Gravity force as:

$$F_g = \frac{\pi d_p^3}{6} \rho_p g \quad (2.25)$$

Where:

$F_g$	Force due to gravity
$d_p$	Particle diameter
$\rho_p$	Particles density
$g$	Acceleration due to gravity

And the buoyancy forces as:

$$F_b = \frac{\pi d_p^3}{6} \rho_f g \quad (2.26)$$

Where:

$F_b$	Buoyancy force
$\rho_f$	Fluid density

For the Hydrodynamic forces, they stated that a particle in a moving fluid experiences a force parallel to the direction of upstream velocity, drag and a force normal to the upstream velocity. These two forces can be obtained based on the definition of the drag coefficient,  $C_D$ , and the lift coefficient,  $C_L$ , [Mingqin Duan, \(2007\)](#).

$$C_D = \frac{F_D}{0.5 \rho_f u^2 A} \quad (2.27)$$



Where:

$C_D$	Drag Coefficient
$u$	phase velocity
$F_D$	Drag force
$A$	Area (ft <sup>2</sup> )

While the lift coefficient is defined as:

$$C_L = \frac{F_L}{0.5 \rho_f u^2 A} \quad (2.28)$$

$C_L$	Lift Coefficient
$F_L$	Lift forces

Zhou, L. (2008), predicted that to initiate rolling of the bed particle, the moments of forces (FB+FL+FD) at the contact point P which tend to cause downstream rotation must be greater than the moments of the force (FG) that tend to prevent downstream rotation. He stated that the condition for initiation of particle rolling at the bed surface is given by:

$$F_L R \sin \theta + F_D R \cos \theta - (F_G - F_B) R \sin(\alpha + \theta) = 0 \quad (2.29)$$

Where  $\alpha$  is the angle of inclination, and  $\theta$  is the angle of repose. The angle of repose is defined as the maximum angle of slope measured from the horizontal plane at which cuttings

come to rest on a pile. It is in the range of 33-38 degrees. Using these, Zhou predicted the critical rolling velocity as:

$$u_{roll} = \sqrt{\frac{4(\rho_c - \rho)gd_p \sin(\alpha + \theta)}{3\rho_L(\sin\theta C_L + C_D)}} \quad (2.30)$$

Where:

$U_{roll}$	Critical velocity for rolling particle
$\theta$	Angle of repose/inclination
$C_L$	Lift Coefficient
$\alpha$	Angle between center point

Also taking the normal and frictional forces at contact points as zero, when the particle lifting is about to occur, then the particle lifting condition at the bed surface is given by the following.

$$F_L - (F_G - F_B) \cos \alpha = 0 \quad (2.31)$$

Where:

$F_L$	Lift forces
$F_G$	Force due to gravity
$F_B$	Buoyancy force
$\alpha$	Angle between center point

By substituting the force equations, Zhou found the critical velocity for particle lifting to be:

$$u_{lift} = \sqrt{\frac{4(\rho_c - \rho_L) g d_p \cos \alpha}{3 \rho_L C_L}} \quad (2.32)$$

Where:

U <sub>lift</sub>	Velocity (critical) for particle lift
-------------------	---------------------------------------

### 2.3 Optimum flow rate for hole cleaning while drilling

The flow rate prediction equations and hole cleaning equations in deviated wells as presented in chapter two of this work and as derived by [Bern et al, \(2006\)](#) is valid only for angles greater than 30 degrees. However, it is possible to produce a model that can be valid for both vertical and deviated wells, by combining the models for the vertical and the deviated, such that the existing deviated charts can be combined with a new chart gotten from the derived model to predict hole cleaning in both near vertical and high angle wells. Hence this chapter will derive hole cleaning model and will also consider the case of washout during drilling.

A model to find equivalent RF (rheology factor) in a vertical section is derived, the angle factor is approximated for a vertical well and a correction factor for the effect of washout in a vertical well is modeled. A model for approximating the rheological factor in vertical sections is derived:

$$RF = \frac{6k}{3585 A_a} \left[ \frac{TI}{Ccl} \right] \quad (2.33)$$

Where:

RF	Rheology factor
CCL	Carrying capacity index
A <sub>a</sub>	Annulus cross sectional area

In the derivation of the above equations, a constant flow rate was assumed in both deviated and vertical formulas, and the well was also assumed to be in gauge, thereby allowing for the use of a constant area. Finally, conditions in both cases were assumed the same.

The use of this equation is very important as will be shown in the next chapter, as it affords us the ability to go to the field with a single set of charts, which could be used for predicting hole cleaning in both vertical and deviated wells. In the approximation of the angle factor (AF) in vertical section, a model is derived thus:

$$\frac{1}{AF} Q_{ver} = Q_{Deviated} \quad (2.43)$$

In the above equation,  $Q_{ver}$  is the flow rate that the well will flow with, if in a vertical well, while  $Q_{Dev}$  is the well's flow rate if in a deviated well, under the same conditions and using the same mud and fluids parameters. Note also that in the above equation, both flow rates are calculated with different formulas, i.e.

$$Q_{vertical} = \frac{400,000 A_a}{\rho k (0.13369)}, \text{ where the area is in } ft^2 \quad (2.35)$$

While,

$$Q_{deviated} = \frac{834.5TI}{\rho RF} \quad (2.36)$$

This is according to the procedure given in the API recommended practice.

Another model showed the equation for predicting correction factors due to hole washout during drilling. The model is derived thus:

$$Q_2 = \left[ \frac{D_2}{D_1} \right]^2 Q_1 \quad (2.37)$$

In the derivation of this equation, it is assumed that  $Q_1$  is the initial critical flow rate when the well was in gauged, while  $Q_2$  is the critical rates needed to clean the well after washout occurs and the well is enlarged.

Furthermore, to come up with a correction factor for the rates, to be able to predict appropriate critical flow rate that can efficiently clean the hole, we had to assume a constant flow velocity, such that a change in the well area affects the effective flow rate needed to maintain a constant velocity that will sufficiently clean the well.

## 2.4 Artificial Intelligence

Artificial intelligence (AI) became one of the most important tools to support the oil and gas drilling industry development (Bello et al. 2016). Recently, artificial neural networks (ANN) have gained widespread popularity in many engineering fields due to its outstanding ability to solve complex and non-linear problems (Naganawa et al. 2014; Razi et al. 2013). The following section gives a briefed idea bout ANN and ANFIS.

### 2.4.1 Artificial Neural Network (ANN)

An artificial neural network (ANN) reflects a similar system to the operations of biological neural networks which is the reason to defined ANN as an emulation of biological neural systems, [Nakamoto \(2017\)](#). ANN's are at the leading edge of computational systems used to produce or at least mimic, intelligent behavior. ANN is capable of resolving paradigms that linear computing cannot process ([Andagoya et al. 2015](#); [Hemphill et al. 2007](#); [Omosebiet al. 2012](#)).

The main processing elements of an ANN system are Neurons. The ANN architecture contains at least three layers (input, hidden and output layer), in addition to a training algorithm and a transfer function, [Lippmann \(1987\)](#). Weights are constants which connect neurons in each layer with the subsequent layer neurons, [Hinton et al. \(2006\)](#). Log-sigmoidal and tan-sigmoidal are the most common transfer functions assigned to hidden layers while 'pure linear' is a commonly used as activation function assigned to the output layer. The input data points go into an ANN model are normalized between -1 and 1 [Niculescu, \(2003\)](#). An ANN model is first trained using a back-propagation of errors while data processing is taking place from the input layer all the way to the output layer. Then a comparison is done between the estimated and the actual data in the output layer. The weights and biases of each layer are updated to match the estimated outputs with the target values. This procedure continues until the error is reduced to the certain acceptable limit as shown in **(Figure 17)** ([Liew et al. 2016](#); [Naganawa et al. 2014](#); [Razi et al. 2013](#)).

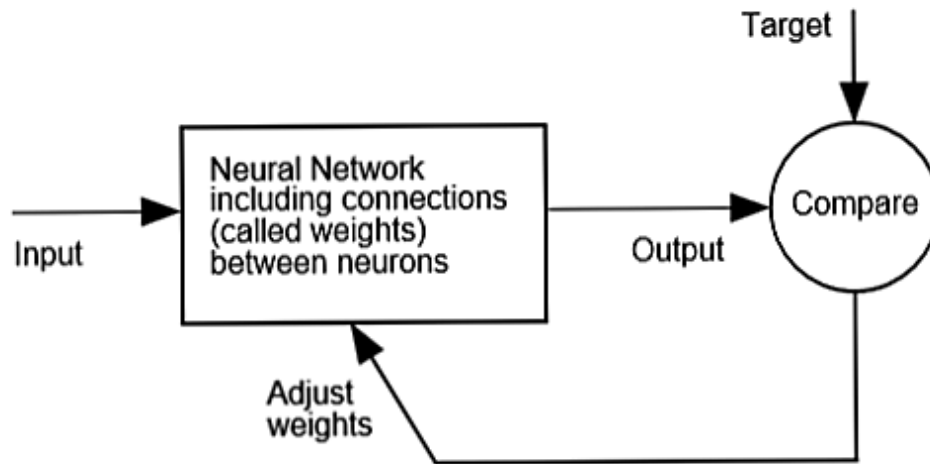


**Figure 17 - ANN System**

Unlike classical AI techniques which directly emulate rational and logical reasoning, neural networks are able to reproduce the underlying processing mechanisms which give rise to intelligence as an emergent property of complex adaptive systems, [Shanmuganathan S. et al. \(2016\)](#). ANN systems have successfully been developed and deployed to solve capacity planning, pattern recognition, intuitive problem-related aspects, robotics, and business intelligence ([Andagoya et al. 2015](#); [Hemphill et al. 2007](#)).

Neural networks gained high interest over the last few years in areas such as data analytics, data mining, and forecasting, [Bharambe M. et al. \(2016\)](#).

## **2.4.2 Adaptive Neuro-Fuzzy Inference System (ANFIS)**

ANFIS is an ANN system based on Takagi–Sugeno fuzzy inference system. This technique was developed in the early 1990s to integrate both fuzzy logic and ANN principles. ANFIS has the potential to combine the benefits of both techniques in a single framework, [Daneshwar, and Noh, \(2013\)](#). Its inference system based on a set of fuzzy IF-THEN rules which can approximate

nonlinear functions and act as a universal estimator, [Shing, and Jang \(1993\)](#). **(Figure 18)** shows an ANFIS architecture composed of four layers of several nodes, [Hamdan and Garibaldi \(2010\)](#). The output of the current layer nodes is served as the input to the next layer nodes After manipulation by the node function in the current layer. During the training process, the training algorithm for ANFIS architecture will tune all the modifiable parameters to match ANFIS with the training data, [Zarandi et al. \(2010\)](#).

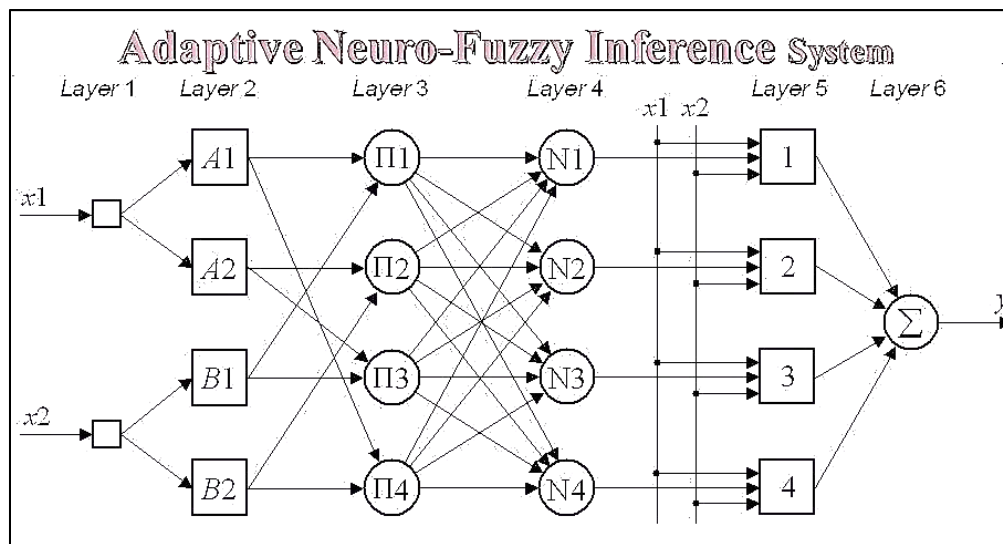


**Figure 18 - Adaptive neuro fuzzy inference system**

In Petroleum Engineering, AI techniques have been utilized for production monitoring, forecasting and multilateral well evaluation ([Olivares et al. 2012](#); [Weiss et al. 2002](#)), PVT parameters prediction ([Alarfaj et al. 2012](#); [Elkatatny 2018a](#)), well integrity evaluation ([Al-Ajmi et al. 2015](#)), assisted history matching ([Al-Thuwaini et al. 2006](#); [Shahkarami et al. 2014](#)), interpreting well logging data and well to well correlation ([Saggaf and Nebrija, 1998](#); [Wu and Nyland, 1986](#); [Lim et al. 1998](#); [Denney 1998](#)), Drilling fluids properties ([Elkatatny 2017](#) ),



reservoir characterization (Kumar et al. 2012), rock mechanics (Sayadia et al. 2013; Elkatatny 2018b) and drilling optimization (Wang and Salehi, 2015).

## 2.5 Equivalent Circulating Density (ECD)

ECD is defined as the sum of the mud hydrostatic pressure and the annulus pressure loss acting on the formation (Haciislamoglu 1994). Factors affect the annular pressure losses (APL) include: annular clearance, mud weight, mud rheology, annular velocity (pump rates), cutting concentration in the annulus, and hole depth.

It can be widely viewed as two main components are affecting the ECD; the cutting portion in the annulus expressed as equivalent static density (ESD), and the mud related parameters (Zhang et al. 2013; Hemphill et al. 2011). Bybee et al 2009 introduced the following equation to predict the ECD:

$$ECD = ESD(1 - C_a) + \left( \rho_s C_a + \frac{\Delta p}{g \cdot 10^{-3} H} \right)^a \quad (2.77)$$

Where, ECD is the equivalent circulating density (g/cm<sup>3</sup>), ESD is the equivalent static density (g/cm<sup>3</sup>),  $C_a$  is the solids concentration in the annular space (%),  $\rho_s$  is the cuttings (solids) density (g/cm<sup>3</sup>),  $\Delta p$  is the pressure losses in the annular space (MPa), H is the well depth along the vertical (m), g is the gravitational acceleration, equal to 9.8 m/s<sup>2</sup>, a is a constant taking into account the measurement units, equal to 8.345.

Such numerical evaluations for predicting ECD values didn't take into account other factors affecting ECD while drilling such as flow geometry defined by well geometry, fluid resistance to

flow defined by fluid rheology, and drill string rotation. Ignoring these factors in the equation will increase the error factors while estimating ECD ([Caicedo et al. 2010](#); [Costa et al. 2008](#)).

Recently in the oil industry, downhole tools are used to measure and monitor changes of ECD and sense its related impact on well control issues ([Erge et al. 2016](#); [Rommetveit et al. 2010](#)). The main tools used now are measurement while drilling (MWD) and pressure while drilling (PWD). These tools contain pressure sensors that can independently measure the bottomhole pressure of the well during drilling, regardless of the factors controlling the ECD ([Ettahadi et al. 2013](#); [Dokhani et al. 2016](#)). The tools can give an accurate reading for ESD and ECD from the total pressure acting on the bottom of the well during circulation. Comparing the ESD with ECD will give a clear view about the reasons for ECD changes ([Vajargah et al. 2016](#); [Osisanya et al. 2005](#); [Lin et al. 2016](#)). In addition to the expensive daily rates of such tools, there are some operating limitations for its application such pressure, temperature, and tool failures.

## CHAPTER 3

### New Hole Cleaning Model

#### 3.1 Methodology

Using a hole cleaning identification parameter called the cutting carrying index (CCI). The CCI, ([Drilling formulas Website](#)) is an empirical relationship from real data which defined as follows:

$$CCI = (k \times AV \times MW) \div (400,000) \quad (3.1)$$

Where;

CCI	Cutting carrying index
AV	Annulus velocity ft/min
MW	Mud weight lb/gal
K	Power law constant

The "400,000" constant was empirically determined by observing hole cleaning conditions on many rigs over an 8- to 10-year period ([Netwas Group Oil Website](#)). The Power Law constant (k) can be calculated from the equation.

$$k = (PV + YP)(511)^{1-n} \quad (3.2)$$

Where;

PV	Plastic viscosity (cP)
YP	Yield point (lb/100ft <sup>2</sup> )
n	Flow behavior index

The flow behavior index (n) can be determined by the following equation:

$$n = 3.322 \log \left( \frac{2PV+YP}{PV+YP} \right) \quad (3.3)$$

[Elkatatny, S. et al. \(2017\)](#) provided a rheological model which will be used in this research to predict on time plastic viscosity and yield point values while drilling.

The Annulus velocity for hole cleaning is a drilling parameter which can be expressed with Larsen's model as the minimum velocity [ $V_{(min)}$ ] is required to lift the cuttings while drilling.

$$V_{(min)} = V_{(cut)} + V_{(slip)} \quad (3.4)$$

[Ozbayoglu, M.E., et al \(2007\)](#) defined this minimum velocity as the summation of the slip velocity and cutting velocity. The cutting velocity depends mainly on the drilling rate of penetration (ROP). The cutting velocity can be expressed as follows:

$$V_{cut} = \frac{ROP}{36 \left[ 1 - \left( \frac{D_{pipe}}{D_{hole}} \right)^2 \right] 0.01778 ROP + 0.505} \quad (3.5)$$

Also, the slip velocity [ $V_{slip}$ ] can be calculated as follows:

$$V_{slip} = \bar{V}_{slip} (C_{ang}) (C_{size}) (C_{mwt}) \quad (3.6)$$

Where:

$$\bar{V}_{\text{slip}} = 0.00516 \mu_a + 3.006 \quad (3.7)$$

$\mu_a$  is the apparent viscosity (cP).

Correlations for mud density, hole angle of inclination and cuttings different sizes should be provided to get the actual annulus velocity as follows:

Mud density correlation factor is:

$$C_{\text{mwt}} = 1 - 0.0333 (\rho_m - 8.7) \quad (3.8)$$

Angle of inclination correlation factor is:

$$C_{\text{ang}} = 0.0342 \theta_{\text{ang}} - 0.000233 \theta_{\text{ang}}^2 - 0.213 \quad (3.9)$$

And cuttings average size correction factor is expressed as:

$$C_{\text{size}} = -1.04D_{50\text{cut}} + 1.286 \quad (3.10)$$

Equivalent circulating density (ECD) will be considered as the effective density in the annulus. A real-time AI model was built to predict ECD values in real-time bases while drilling using surface data.

The new hole cleaning model is called the hole cleaning index (HCI) and will have the following form:

$$HCI = \frac{1}{6666.66667} [X * (Y + Z) * ECD] \quad (3.11)$$

Where:

$$X = \left( (PV + YP)(511)^{1 - \left( 3.322 \log \left( \frac{2PV + YP}{PV + YP} \right) \right)} \right) \quad (3.12)$$

$$Y = \left( \frac{ROP}{36 \left[ 1 - \left( \frac{D_{pipe}}{D_{hole}} \right)^2 \right] 0.01778 ROP + 0.505} \right) \quad (3.13)$$

$$Z = \left[ (0.00516 \mu_a + 3.006) * (0.0342 \theta_{ang} - 0.000233 \theta_{ang}^2 - 0.213) \right. \\ \left. * (-1.04 D_{50cut} + 1.286) * (1 - 0.0333 (ECD - 8.7)) \right] \quad (3.14)$$

**Table 4 - HCI Parameters Identification**

Parameter	Name	Dimensions
PV	Plastic Viscosity	cP
YP	Yield Point	Lb/100ft <sup>2</sup>
ROP	Rate of Penetration	ft/hr
D <sub>pipe</sub>	Drill Pipe Diameter	inch
D <sub>hole</sub>	Hole Diameter	inch
μ <sub>a</sub>	Apparent Viscosity	cP
θ <sub>ang</sub>	Hole Inclination	Degree
D <sub>50cut</sub>	Average Particle Size	Micron
ECD	Equivalent Circulating Density	ppg

### 3.2 Equivalent circulating density (ECD) prediction using Artificial Intelligence (AI)

To build an AI model using ANN and ANFIS techniques, inputs and output had to be defined. In this dissertation, the following surface parameters were used as inputs for an AI model: rate of penetration (ROP), mud weight going into the hole (MWI), drill pipe pressure (DPP).

The reason these parameters were called (surface), is they can be measured from the surface without downhole measurements. By looking to these three input parameters, it will be noticed that all other drilling parameters affecting ECD values are related to one or more of these three parameters. More than 3000 data point of previous mentioned parameters were collected from drilling 8.5” section in an oil well.

In order to have an accurate prediction from the use of AI techniques, data should be filtered and analyzed before being used in the AI model. Filtration process starts with removing all random values that cannot represent the measurements such as negative values, 999 values and null ones ([Andagoya et al. 2015](#); [Hemphill et al. 2007](#); [Omosebiet al. 2012](#)). Second process of filtration was the use of histogram plot to remove the data out layers. To use histogram over the three input parameters will not be effective as it might remove useful data, so using histogram over one parameter will filter the data in more efficient way. From an engineering point of view, ROP values will be the suitable parameter to be used in histogram plotting filtration process. The initial histogram plot for ROP values had shown out layer over 30 m/hr value as shown in (**Figure 19**).

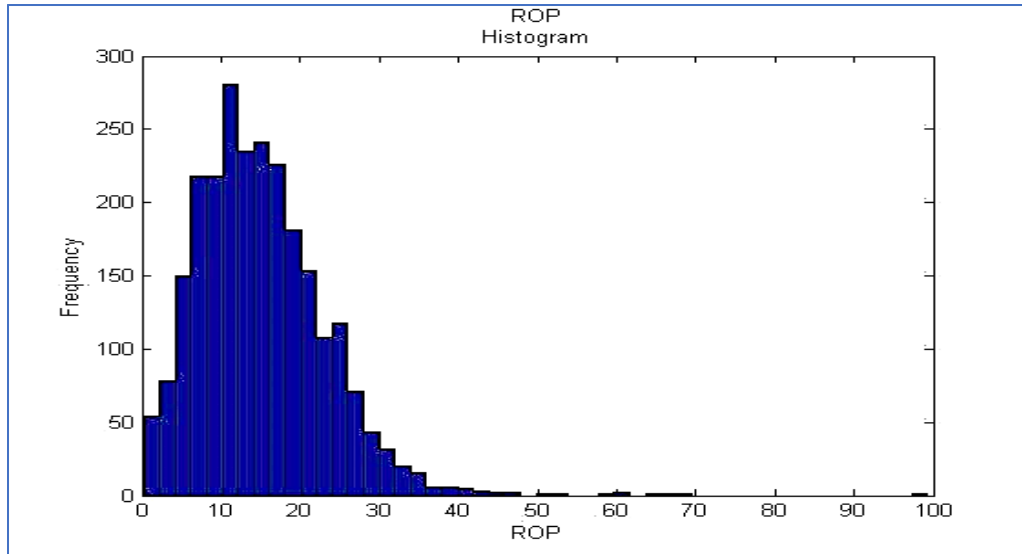


Figure 19 - ROP histogram before filtering

After removing ROP out layer values greater than 30 m/hr, 2376 data points remained, and the histogram plot changed to (Figure 20).

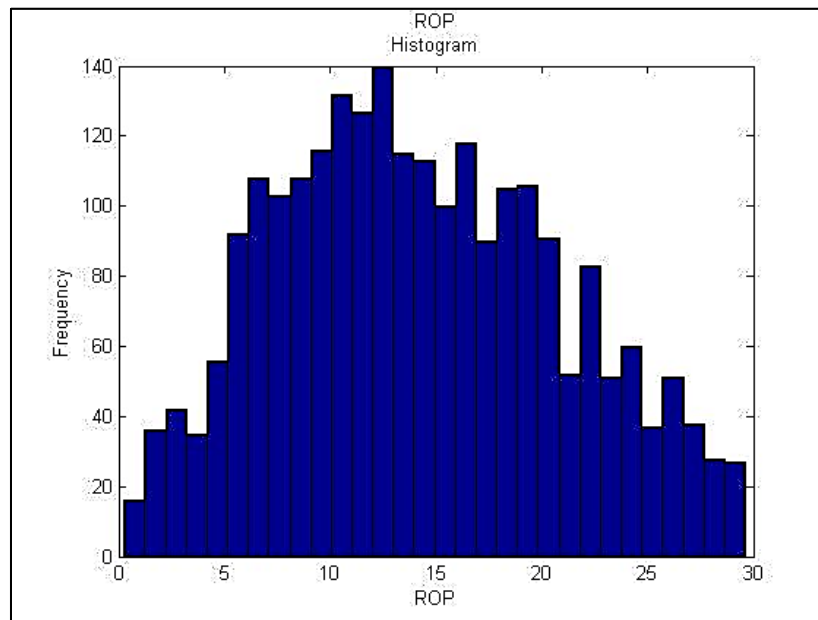


Figure 20 - ROP histogram after filtration

To ensure how effective is the filtration process on the quality of the data to be used AI model, data analyzing using statistics was done as shown in **Table 5**. These results for statistical analysis for the inputs values showing good quality for the data



arrangement and variation which means that we can use it for accurate prediction for ECD values using AI techniques.

**Table 5 - Statistics Analysis of the used data set**

	ROP	MWI	DPP
Max.	29.62	12	6920.04
Min.	0.26	10.5	4945.85
Mean	14.19	11.09	5873.93
Mode	22.6	10.5	5634
Range	29.36	1.5	1974.19
Skewness	0.21	0.43	0.33
Coefficient	0.47	0.06	0.08

### **3.2.1 First ECD Model – ANN:**

Multiple layered neural network model was created with three layers. The 2376 data points representing ROP, MWI & DPP as inputs were randomly used as following:

- 70% for training the network.
- 15% for testing the results.
- 15% to validate the network results.

(Figure 21) shows the training and testing results of predicting ECD values, while (Figure 22) is showing the predicted ECD profile of booth ANN training and testing.

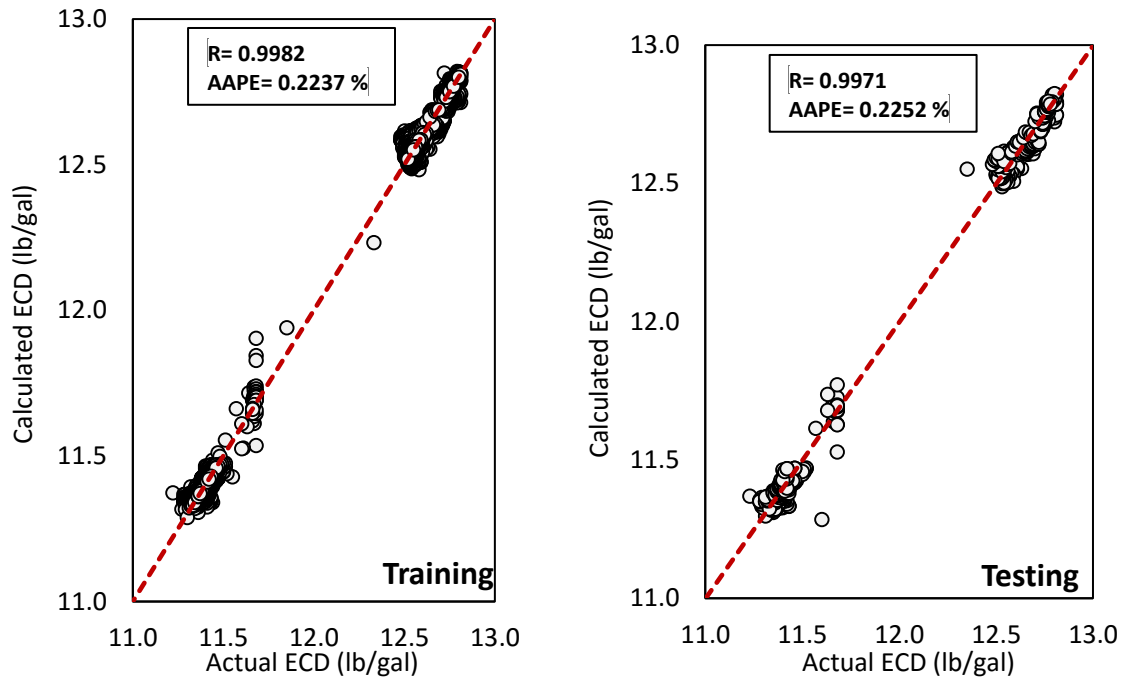


Figure 21 - Predicted ECD for booth ANN training and testing compared with Field measurement

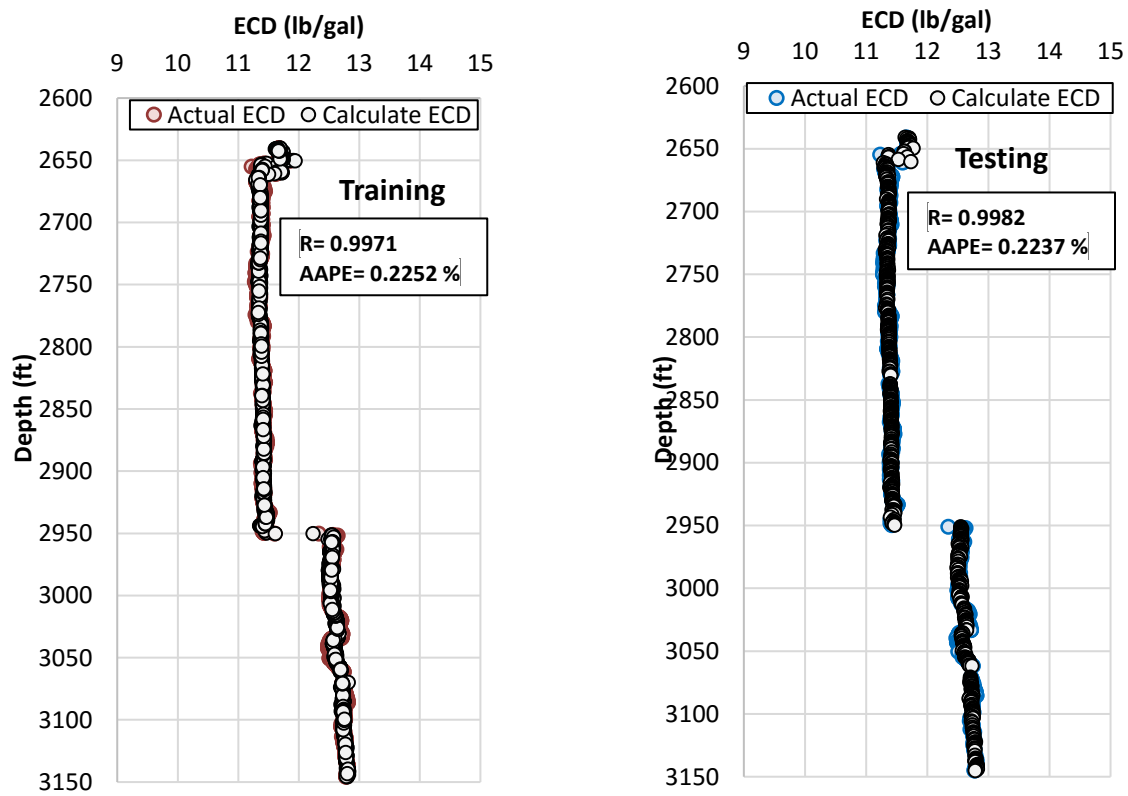


Figure 22 - ECD profile of booth ANN model training and testing compared with ECD from field measurement

Significant results were obtained for real predicted ECD values (**Table 6**), this was shown from using correlation coefficient and average absolute error percent (AAPE) (Janjua et al. 2011; Diaz wt al. 2004) terms to check prediction accuracy as follows:

**Table 6 - ANN model training and testing Correlation Coefficient and AAPE**

Parameter	Training	Testing
Correlation Coefficient	0.9971	0.9982
Average absolute percentage error (%)	0.2252	0.2237

### 3.2.2 Second ECD Model – ANFIS

An ANFIS model was created using 5 membership functions, using gaussmf as input membership function, and linear as output membership function with a random selection of training and testing data points. (**Figure 23**) shows the training and testing results which have a good match with the measure ECD values. Also, the ECD-depth profile showed the high accuracy of the training and testing results (**Figure 24**) with high correlation coefficient and AAPE as shown in **Table 7**.

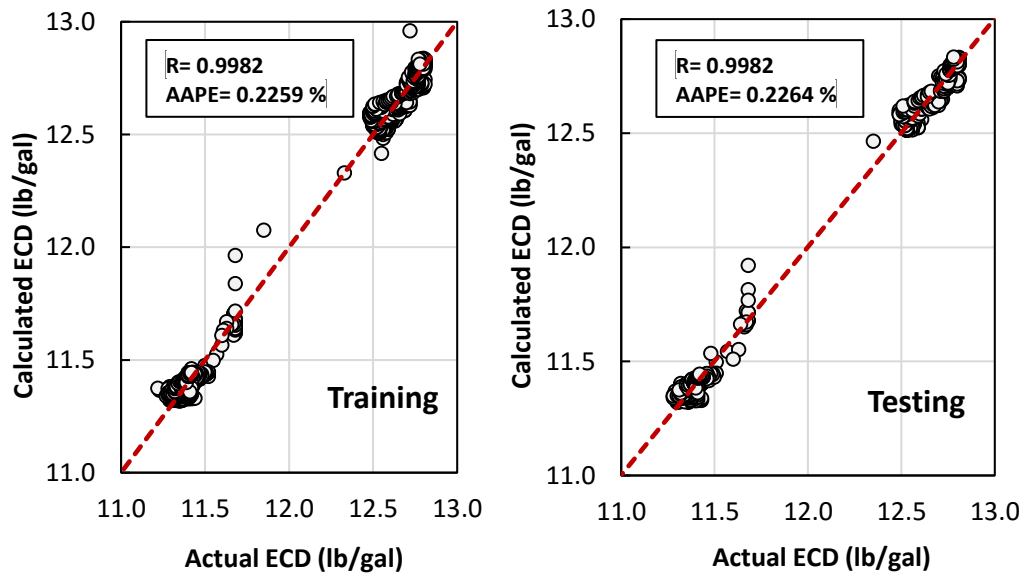


**Figure 23 - Predicted ECD from ANFI Model (training and testing) compared with field measurement.**

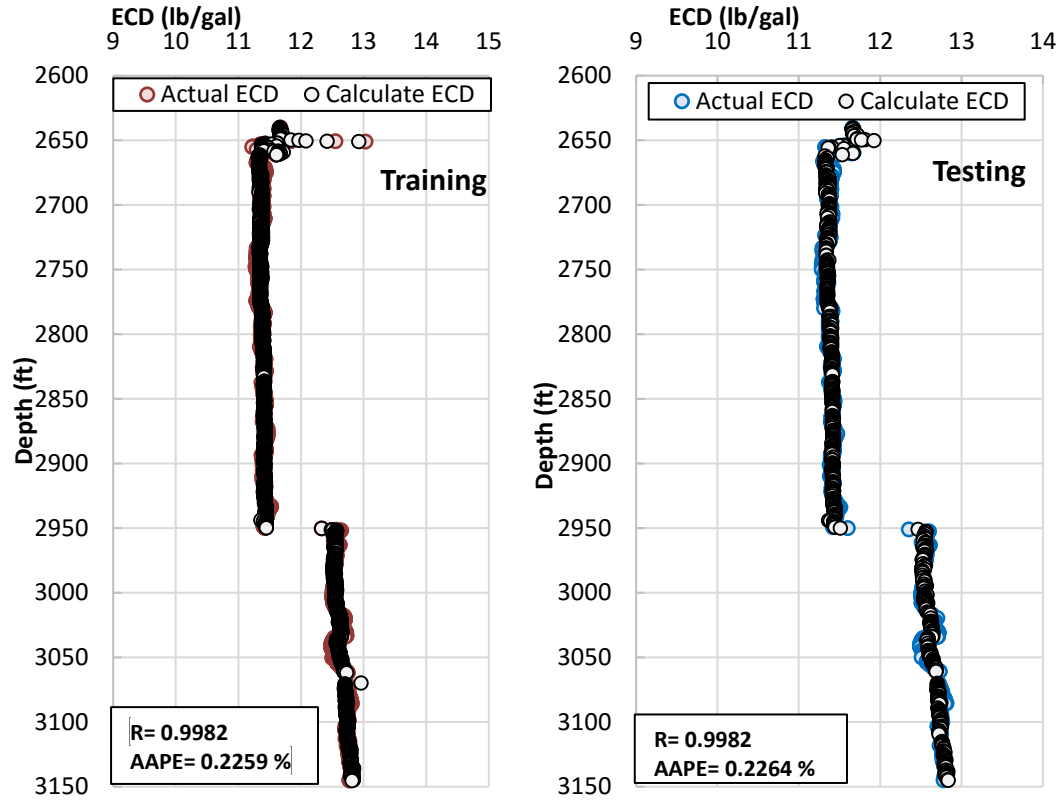


**Figure 24 - ECD profile of booth ANFIS model training and testing compared with ECD from field measurement**

**Table 7 - ANFIS model training and testing Correlation Coefficient and AAPE**

Parameter	Training	Testing
Correlation	0.9982	0.9982
Average	0.2258	0.2262

As the results of these two models were highly accurate with an error factor of 0.22 %, hence, one of the two ECD models will be used to predict ECD values while drilling with surface data without the need for measurement while drilling (MWD) downhole tools. These on-time ECD values will be used in the main hole cleaning model (HCI) to accurately matching the hole conditions while drilling.

### 3.3 Mud Rheology prediction using Artificial Intelligence

As an extension of [Salaheldin et al., \(2016\)](#) rheological model on invert emulsion-based drilling fluid, an artificial intelligence model was built to predict drilling fluid yield point, plastic viscosity, and apparent viscosity. Data range has been collected for oil base mud to be used model building and verification.

The drilling fluid (mud) density is measured using the mud balance frequently on the rig. The drilling fluid rheological properties (yield point and plastic viscosity) are measured in the mud lab using the rheometer at 120°F ([Elkatatny et al., 2012](#), [Power and Zamora, 2003](#); and [Maxey, 2007](#)). On the rig, the derrick man measures the Marsh funnel viscosity every 15 mins while drilling at room temperature.

A number of 576 samples were collected and drilling fluid density, Marsh funnel viscosity and solid volume content was measured. In order to have accurate AI model, data will need to be filtered and analyzed before being used in the AI technology. Filtration process starts with removing all random values that cannot represent the measurements such as negative values, 999 values and null ones ([Andagoya et al. 2015](#); [Hemphill et al. 2007](#); [Omosebiet al. 2012](#)). The second process of filtration was the use of a histogram plot to remove the data out layers. To use histogram over the three input parameters will not be effective as it might remove useful data, so using histogram over one parameter will filter the data in more efficient way. From an engineering point of view, Marsh funnel viscosity values will be the suitable parameter to be used in histogram plotting filtration process. The initial histogram plot for Marsh funnel viscosity values had shown out layer over 100 cP value as shown in (**Figure 25**).

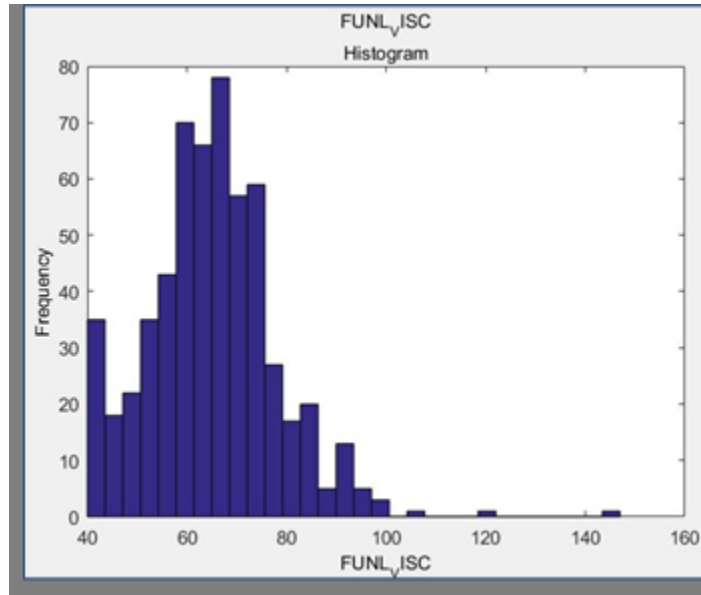


Figure 25 - Initial marsh funnel viscosity Histogram

After removing Marsh funnel viscosity out layer values greater than 100 cP, 421 data points remained and the histogram plot changed to (Figure 26).

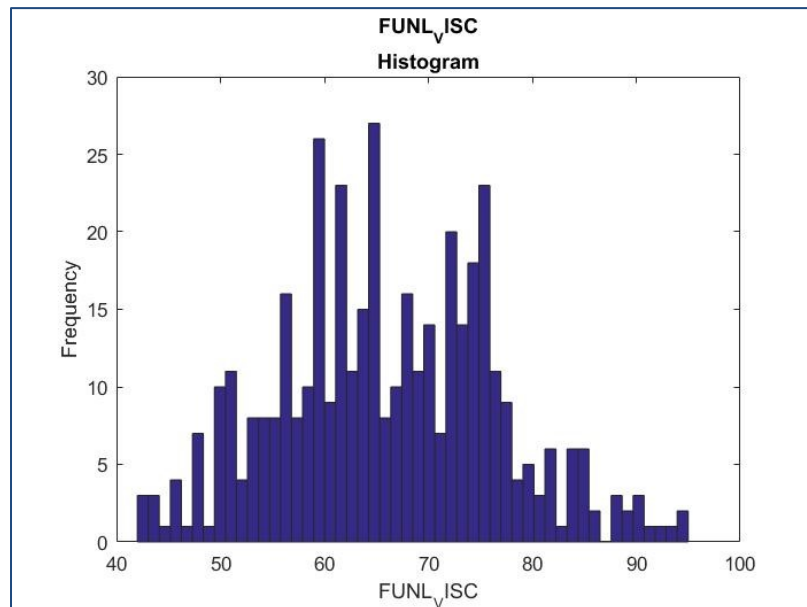


Figure 26 - Final Marsh funnel viscosity Histogram

To ensure how effective is the filtration process on the quality of the data to be used AI model, data analyzing using statistics was done as shown in **Table 8**. These results for statistical analysis for the inputs values showing good quality for the data arrangement and variation which means that we can use it for accurate prediction for oil-base mud rheological properties using AI techniques.

**Table 8 - Statistics Analysis of the used data set**

	Mud wt	Marsh/funnel_Vis	Solid_Vol
Max.	100	95	25
Min.	66	42	9
Mean	81.17	66.08	15.95
Range	34	53	15
Skewness	0.24	0.14	0.19
Coefficient	0.99	0.11	0.18

### 3.3.1 First Rheological Model – ANN

Multiple layered neural network model was created with three layers. The 421 data points representing mud wt, funnel vis and solid volume as inputs were randomly used as following:

- 70% for training the network.
- 15% for testing the results.
- 15% to validate the network results.

(**Figure 27**) shows the training results of predicting yield point values using ANN model.

(**Figure 28**) shows the testing results of predicting yield point values using ANN model.

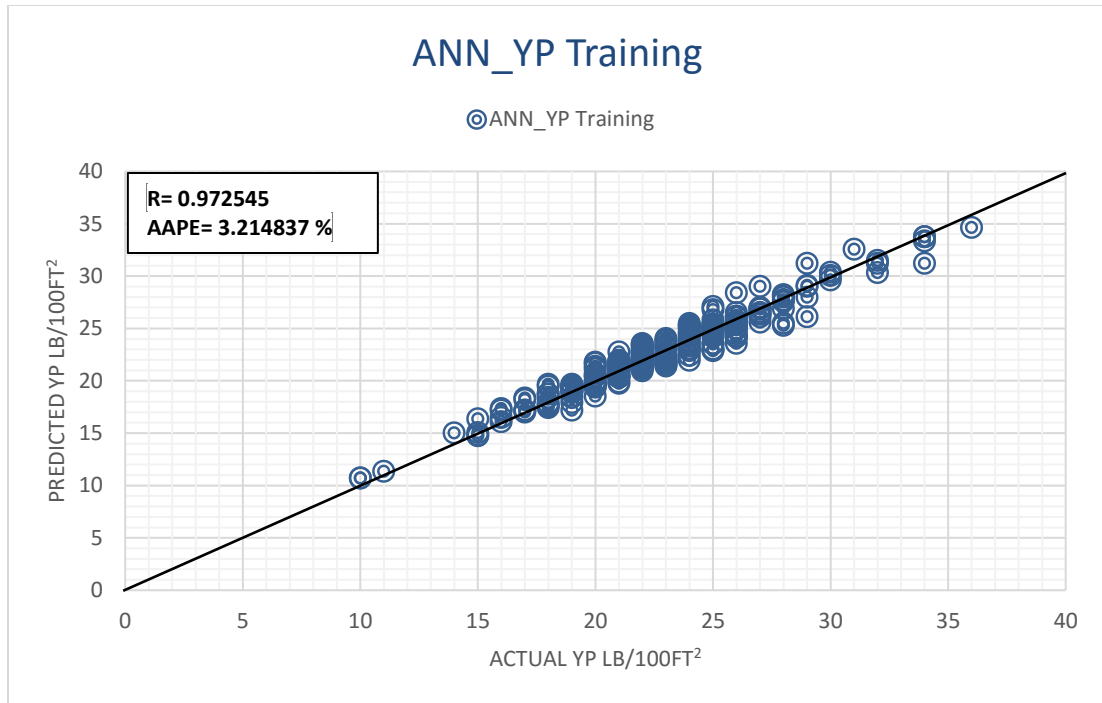


**Figure 27 - Predicted YP from ANN Model compared with field measurement (training results)**

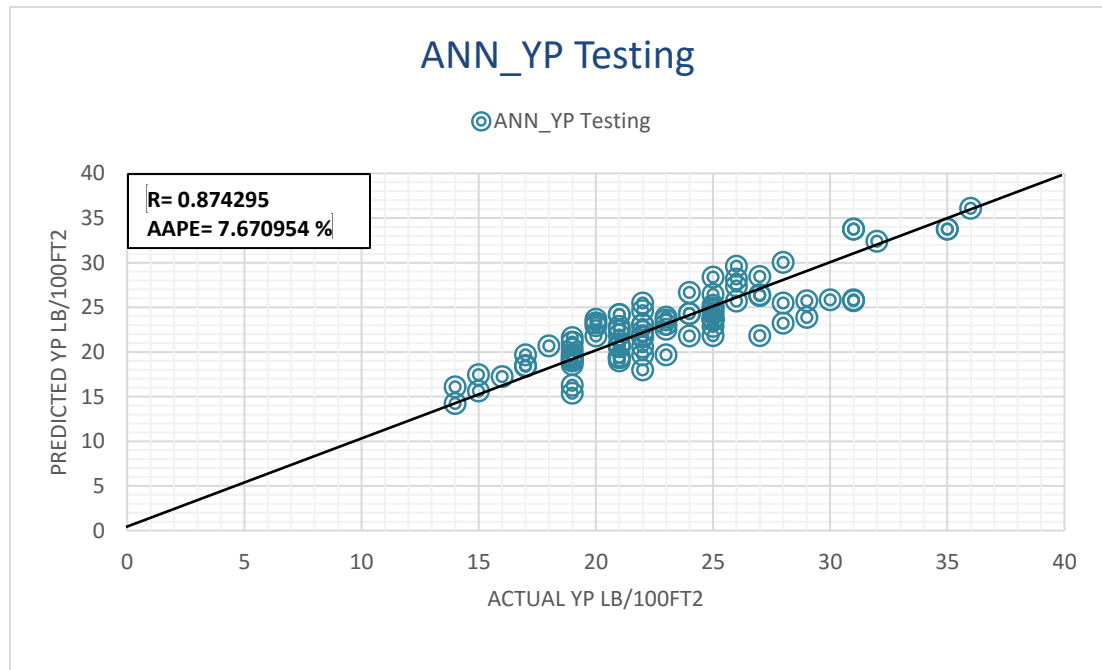


**Figure 28 - Predicted YP from ANN Model compared with field measurement (testing results)**

(Figure 29) shows the training results of predicting plastic viscosity values using ANN model. (Figure 30) shows the testing results of predicting plastic viscosity values using ANN model.



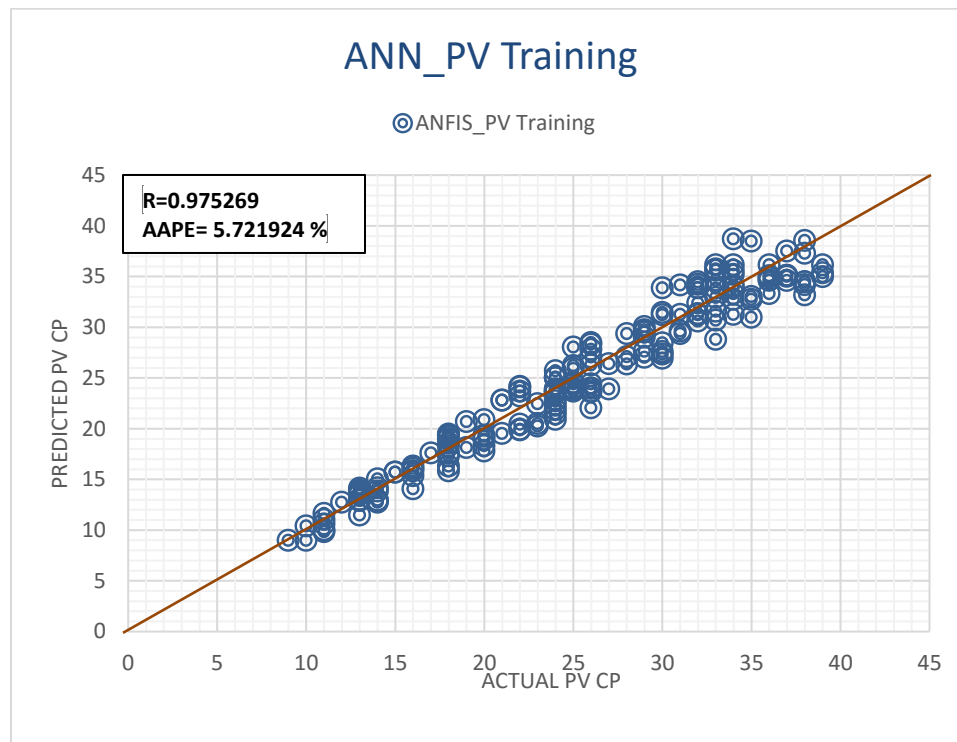


Figure 29 - Predicted PV from ANN Model compared with field measurement (training results)

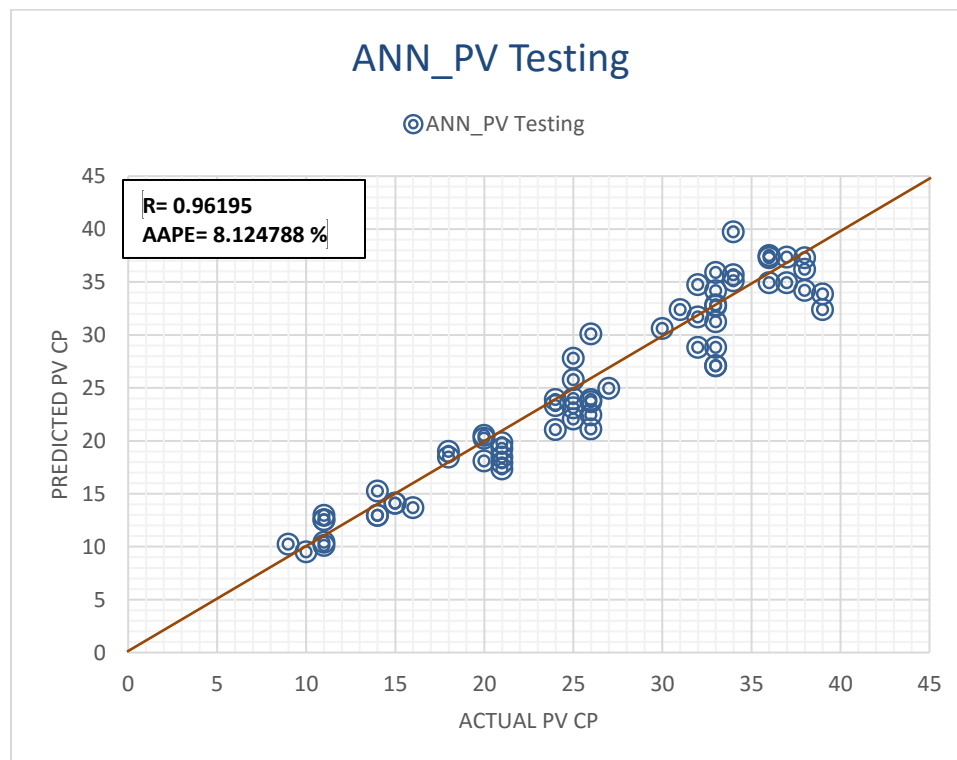


Figure 30 - Predicted PV from ANN Model compared with field measurement (testing results)

(Figure 31) shows the training results of predicting apparent viscosity values using ANN model. (Figure 32) shows the testing results of predicting apparent viscosity values using ANN model.

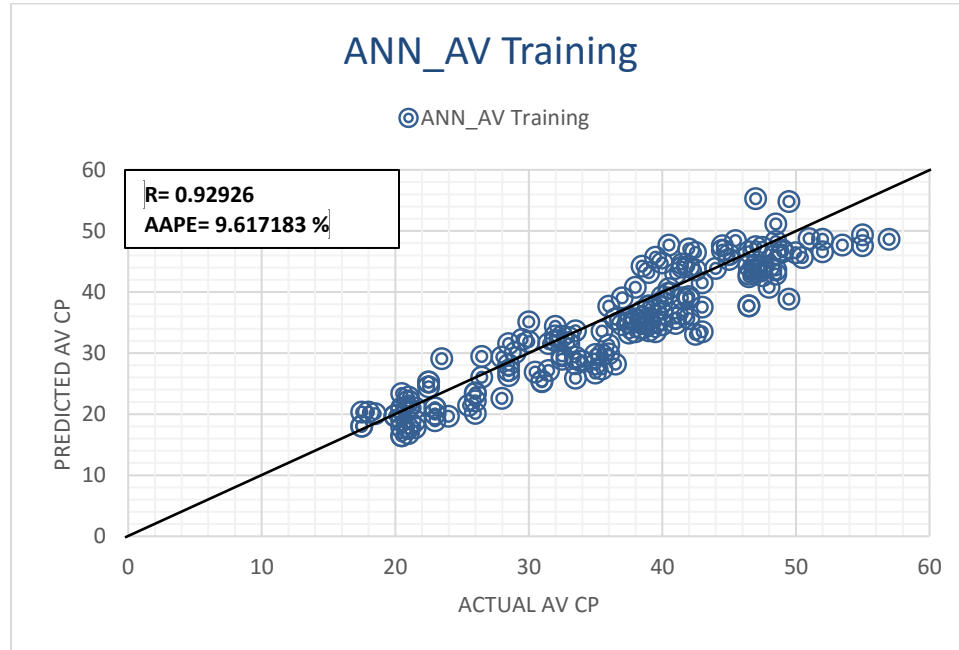


Figure 31 - Predicted AV from ANN Model compared with field measurement (training results)

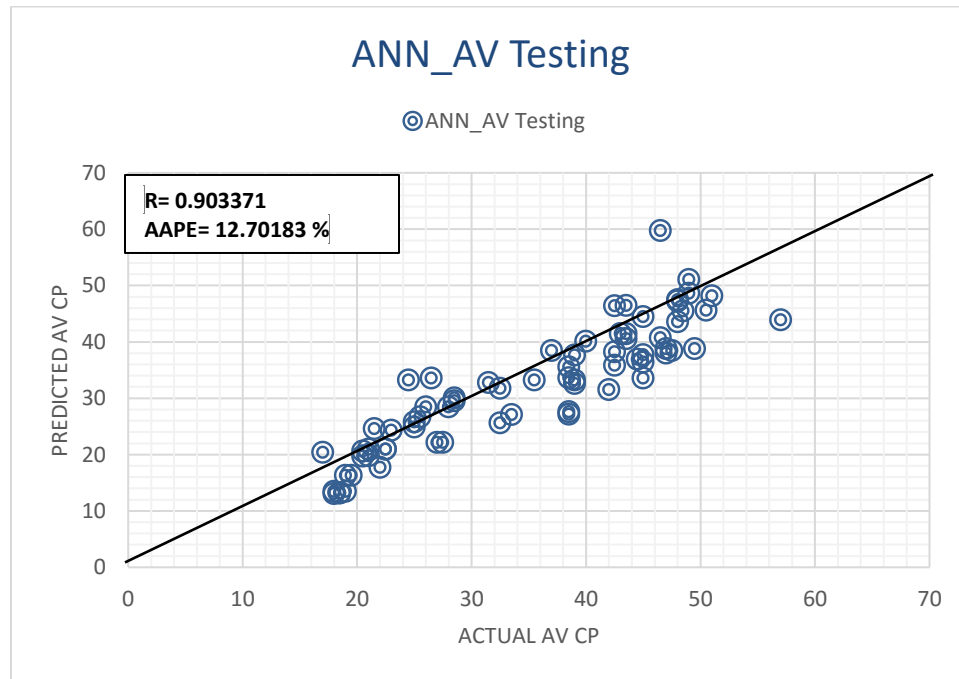


Figure 32 - Predicted AV from ANN Model compared with field measurement (testing results)

Significant results were obtained for predicted rheological properties (**Table 9**), this was shown from using correlation coefficient and average absolute error percent (AAPE) (Janjua et al. 2011; Diaz wt al. 2004) terms to check prediction accuracy as follows:

**Table 9 - ANN rheological model training and testing Correlation Coefficient and AAPE**

Parameter	Correlation Coefficient (Training)	Correlation Coefficient (Testing)	Average absolute percentage error (%) - Training	Average absolute percentage error (%) - Testing
Yield Point (YP)	0.97	0.87	3.2	7.67
Plastic Viscosity (PV)	0.975	0.962	5.72	8.12
Apparent Viscosity (AV)	0.93	0.90	9.6	12.7

### 3.3.2 Second Rheological Model – ANFIS

An ANFIS model was created using 5 membership functions, using gaussmf as input membership function, and linear as output membership function with random selection of training and testing data points.

(**Figure 33**) shows the training results of predicting yield point values using ANFIS model. (**Figure 34**) shows the testing results of predicting yield point values using ANFIS model.

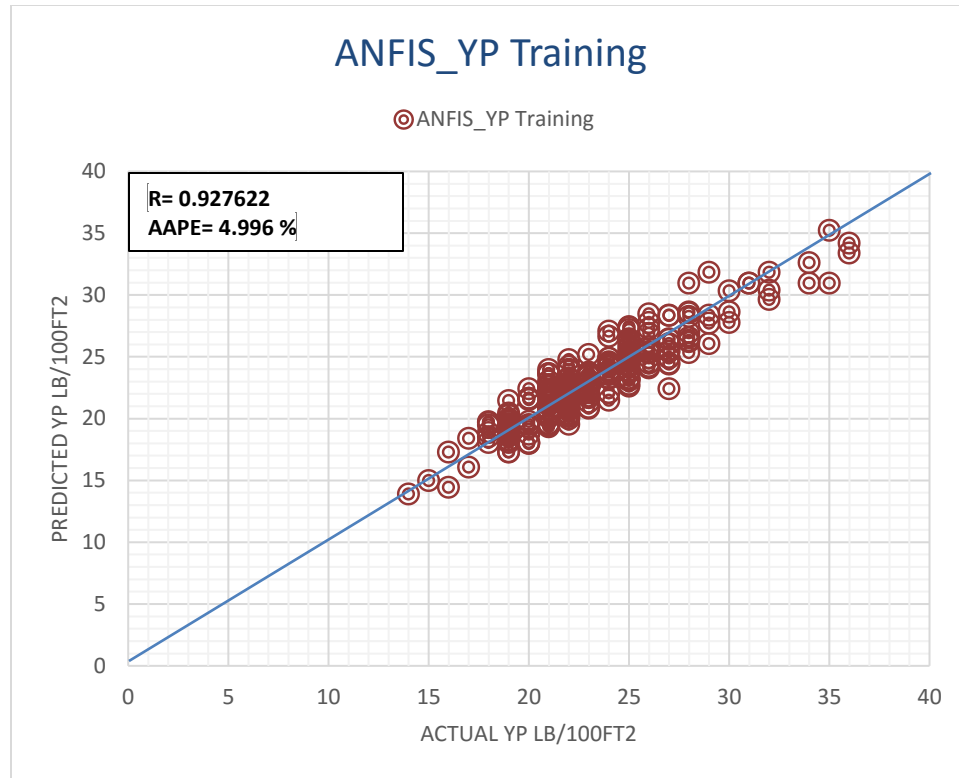


Figure 33 - Predicted YP from ANFIS Model compared with field measurement (training results)

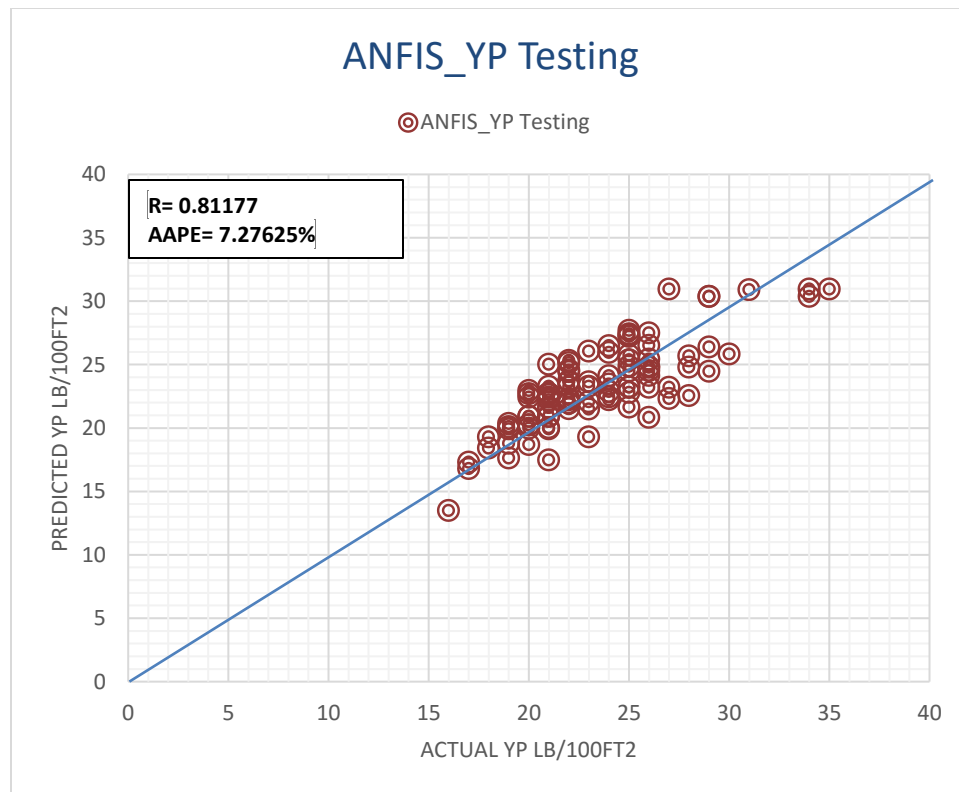


Figure 34 - Predicted YP from ANFIS Model compared with field measurement (testing results)

(Figure 35) shows the training results of predicting plastic viscosity values using ANFIS model. (Figure 36) shows the testing results of predicting plastic viscosity values using ANFIS model.

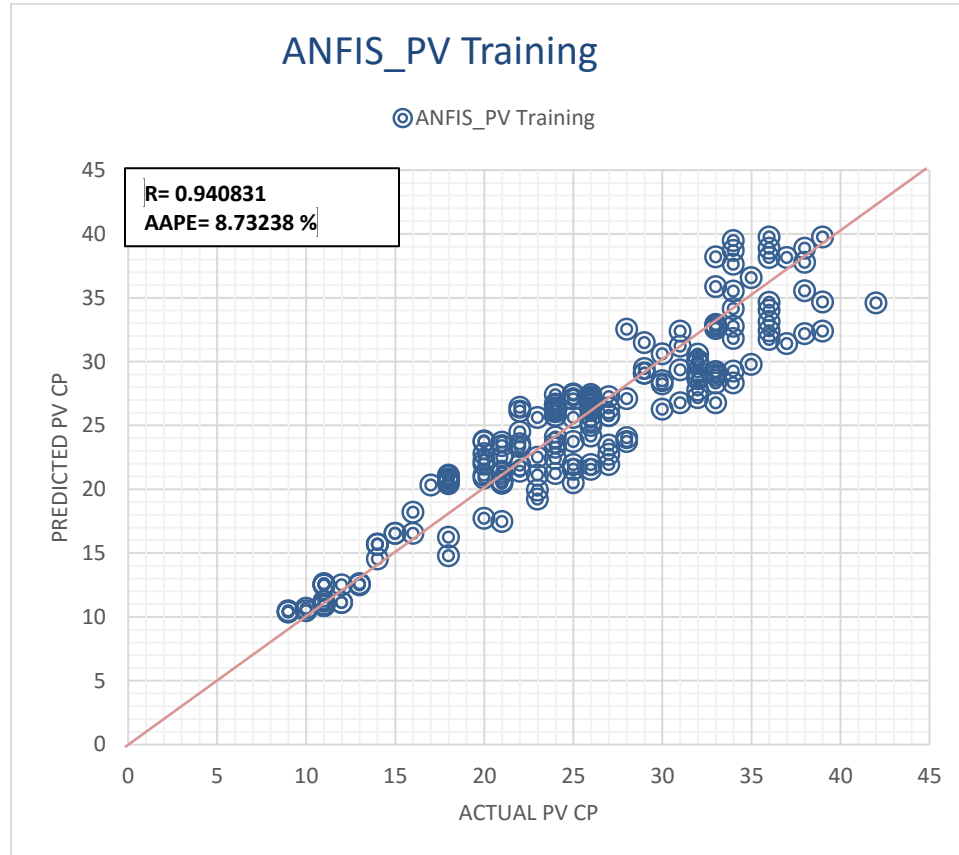
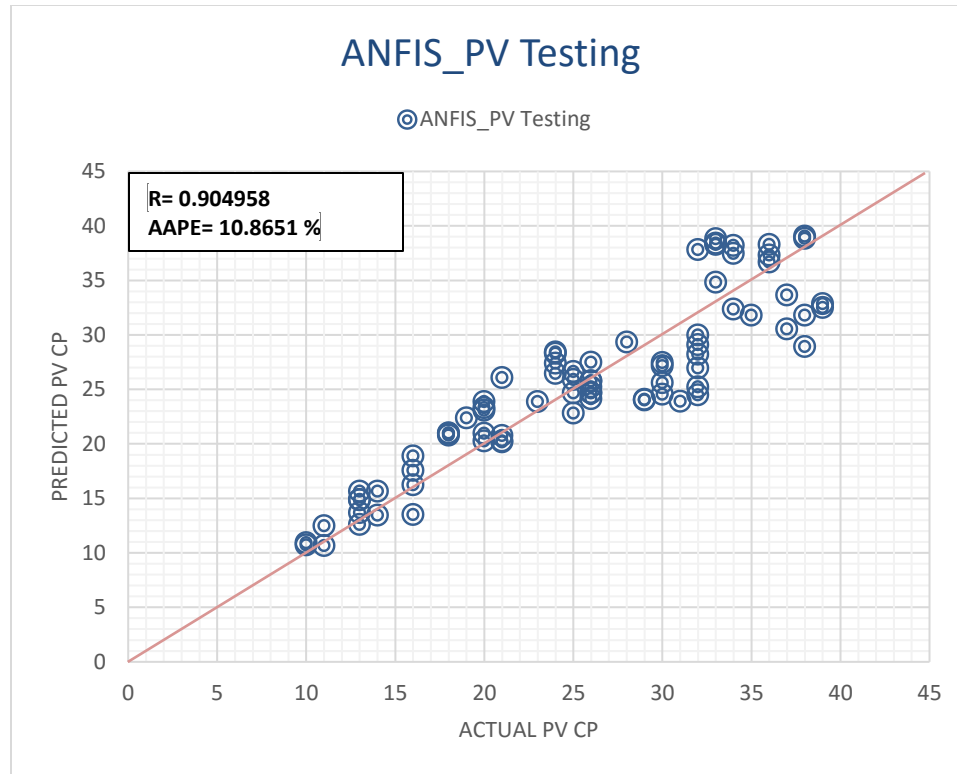


Figure 35 - Predicted PV from ANFIS Model compared with field measurement (training results)



**Figure 36 - Predicted PV from ANFIS Model compared with field measurement (testing results)**

(**Figure 37**) shows the training results of predicting apparent viscosity values using ANFIS model. (**Figure 38**) shows the testing results of predicting apparent viscosity values using ANFIS model.

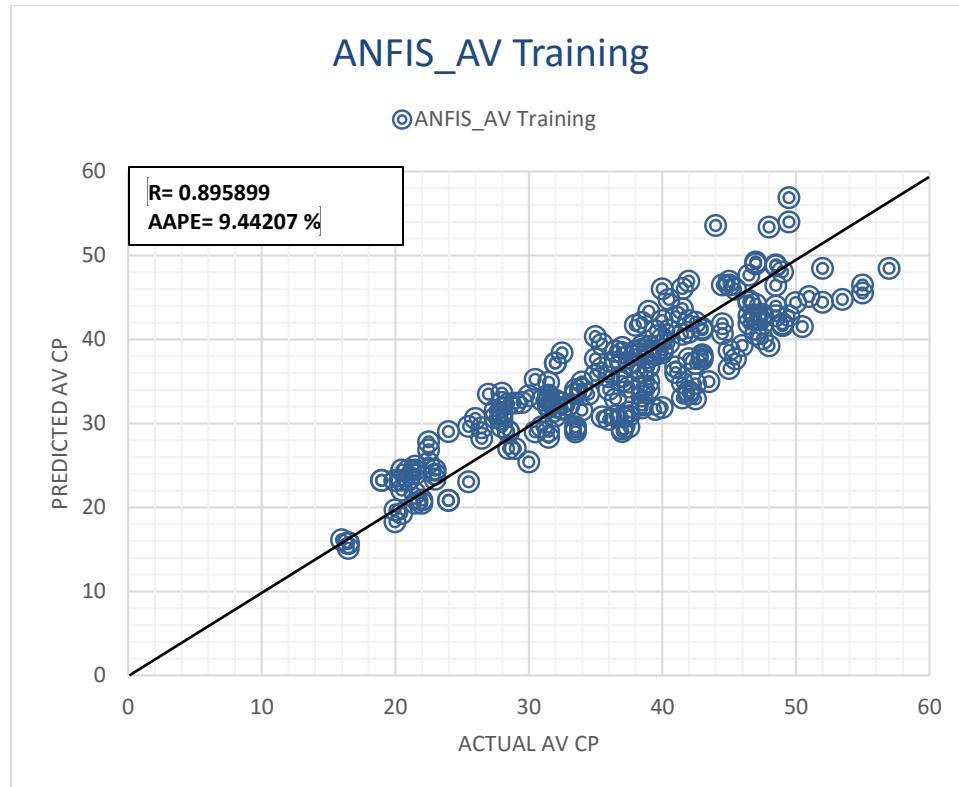


Figure 37 - Predicted AV from ANFIS Model compared with field measurement (training results)

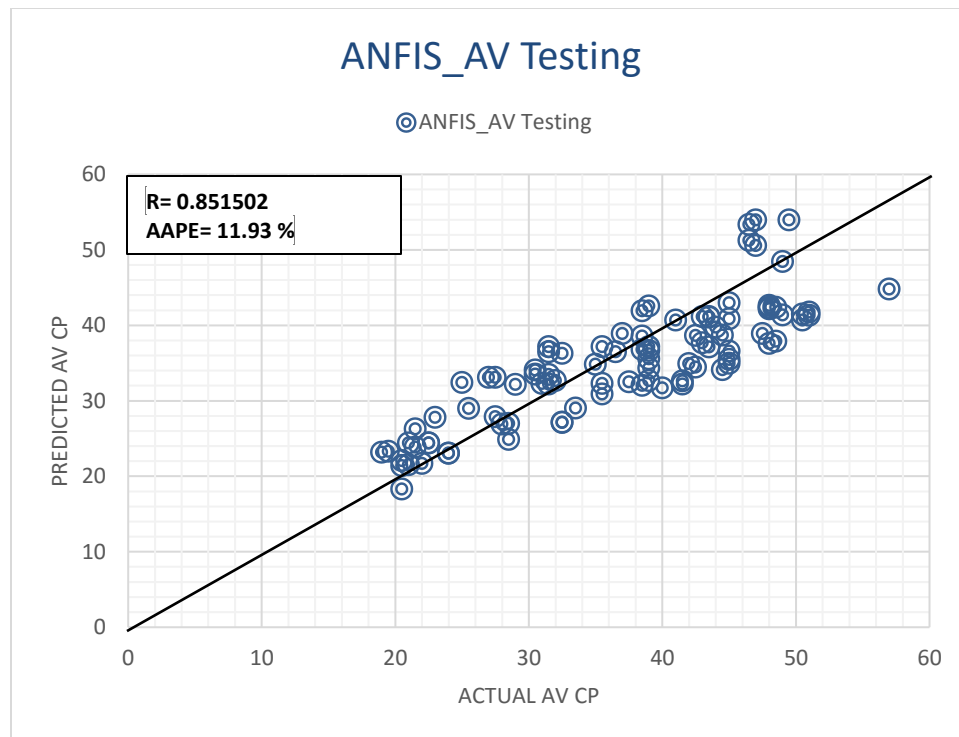


Figure 38 - Predicted AV from ANFIS Model compared with field measurement (testing results)

(Table 10) is showing the results related to OBM mud rheological properties prediction using AI ANFIS model.

**Table 10 - ANFIS rheological model training and testing Correlation Coefficient and AAPE**

Parameter	Correlation Coefficient (Training)	Correlation Coefficient (Testing)	Average absolute percentage error (%) - Training	Average absolute percentage error (%) - Testing
Yield Point (YP)	0.93	0.81	4.996	7.27
Plastic Viscosity (PV)	0.94	0.90	8.7	10.87
Apparent Viscosity (AV)	0.896	0.85	9.44	11.93

As the results of these two models were highly accurate with max average absolute percentage error (AAPE) 0.32%, hence, one of the two rheological models will be used to predict YP, PV and AV values while drilling with surface data without the need for measurement while drilling (MWD) downhole tools. These on-time rheological values will be used in the main hole cleaning model (HCI) to accurately matching the hole conditions while drilling.



## CHAPTER 4

### RESULTS AND CONCLUSIONS

#### 4.1 Hole Cleaning Efficiency (HCI)

To build a reliable hole cleaning model, field considerations were highly concerned. A huge challenge was faced to collect the proper range of field data which can cover the need for model development and verification. 135 measured set data points (**Table 11**) were collected from an oil well being drilled in north Africa. These data points had been used to feed the ECD AI model, the mud rheological AI model and the final HCI model.

The chosen field data belong to a drilled well which faced a serious down hole stuck situation. Indicators were there – downhole – but these indications were not recognized on the surface. By using the developed HCI model in this dissertation, rig crew members on the surface will be able to define the hole cleaning problem once happen downhole and so they can take the corrective remedial actions to avoid worst stuck pipe scenarios.

As part of this study, developed HCI software will be provided. Using the surface drilling parameters as inputs and provides an on-time alert on surface once the downhole cleaning conditions become crucial. The main HCI model development will be divided into three stages.

Table 11 - Part of the real drilling parameters – Oil well in north Africa

Depth ft	ROP ft/hr	MWI (ppg)	DPP (psi)	ECD (ppg)	FUNL_VISC (cP)	SOLID_VOL (%)	Hole inclination	Average cutting size (D 50cut) (mm)	Pipe Diameter (in)	Hole Diameter (in)	PV (cP)	YP (lb/100ft <sup>2</sup> )	AV (cP)
32.8	45.92	8.76	160	8.77	78	4.00	0.0086124	3.057	5	23	22	38	52.56
656	49.20	8.84	650	8.85	71	5.00	0.1722488	3.122	5	23	24	37	45.61
685.52	45.92	8.83	660	8.84	71	4.00	0.18	2.020	5	16	22	24	45.56
780.64	45.92	8.84	670	8.86	70	5.00	1.06	2.890	5	16	23	27	44.55
875.76	45.92	8.84	700	8.85	70	6.00	3.96	3.720	5	16	22	24	44.55
1062.72	42.64	8.85	750	8.87	70	5.00	11.61	0.503	5	16	23	24	44.6
1157.84	42.64	8.6	760	8.7	71	3.00	13.72	0.786	5	16	22	24	44.38
1249.68	45.92	8.7	780	8.75	72	4.00	14.42	1.100	5	16	24	25	45.94
1348.08	49.20	8.8	820	8.84	71	7.00	14.51	0.950	5	16	21	26	45.41
1439.92	55.76	8.8	850	8.9	70	5.00	16.88	0.800	5	16	20	26	44.35
1535.04	49.20	8.9	880	8.96	71	6.00	19.61	0.600	5	16	21	26	45.92
1626.88	45.92	8.9	950	8.97	71	5.00	20.84	0.800	5	16	22	26	45.92
1722	45.92	8.9	1000	8.97	70	6.00	23.57	0.900	5	16	23	24	44.86
1817.12	55.76	8.9	1100	8.99	70	8.00	24.62	0.850	5	16	22	24	44.86

#### 4.1.1 Stage 1 – ECD Prediction

Multiple layered neural network model was created with three layers. The 135 data points representing ROP, MWI & DPP as inputs were randomly used as following:

- 70% for training the network.
- 15% for testing the results.
- 15% to validate the network results.

(Figure 39) shows the training results of predicting ECD values, while (Figure 40) is showing the testing results of predicting ECD values using ANN model.

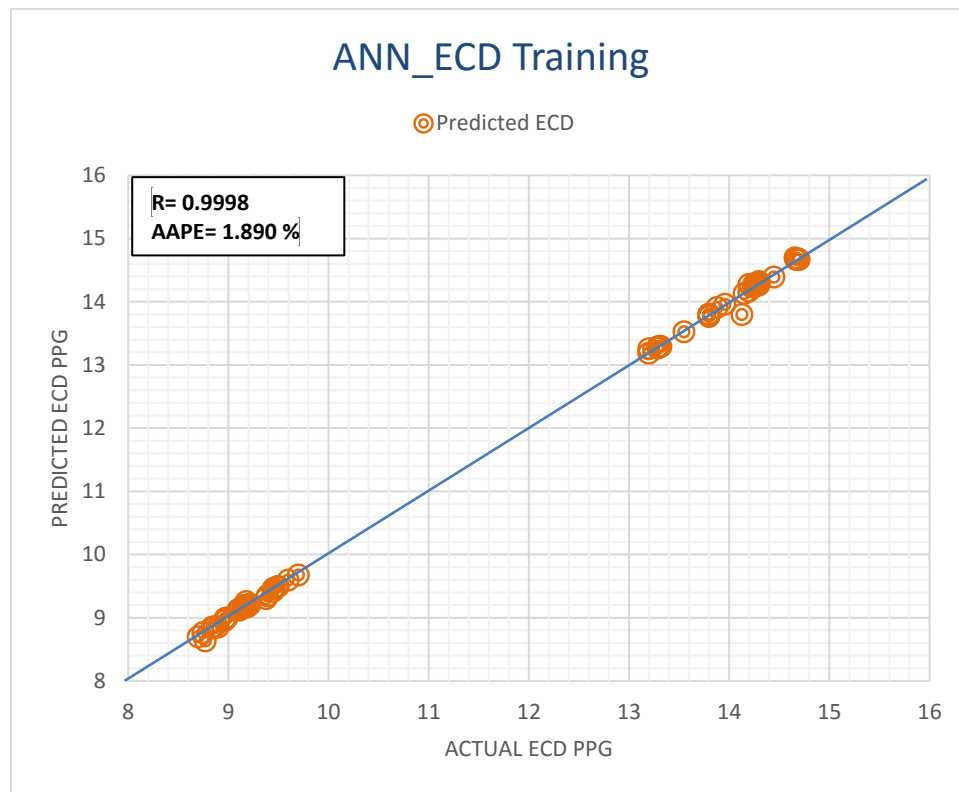
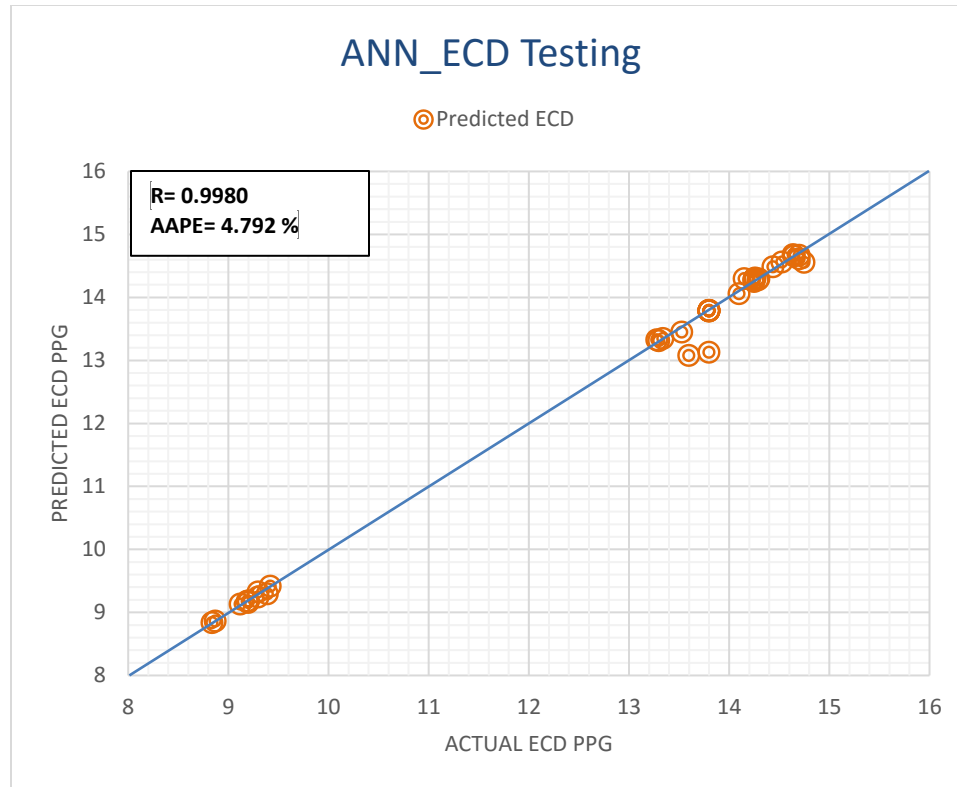


Figure 39 - Predicted ECD from ANN Model compared with field (training)



**Figure 40 - Predicted ECD from ANN Model compared with field (testing)**

(**Figure 41**) is showing the predicted ECD profile resulting from training the ANN model. Also, (**Figure 42**) is showing the predicted ECD profile resulting from testing the ANN model.

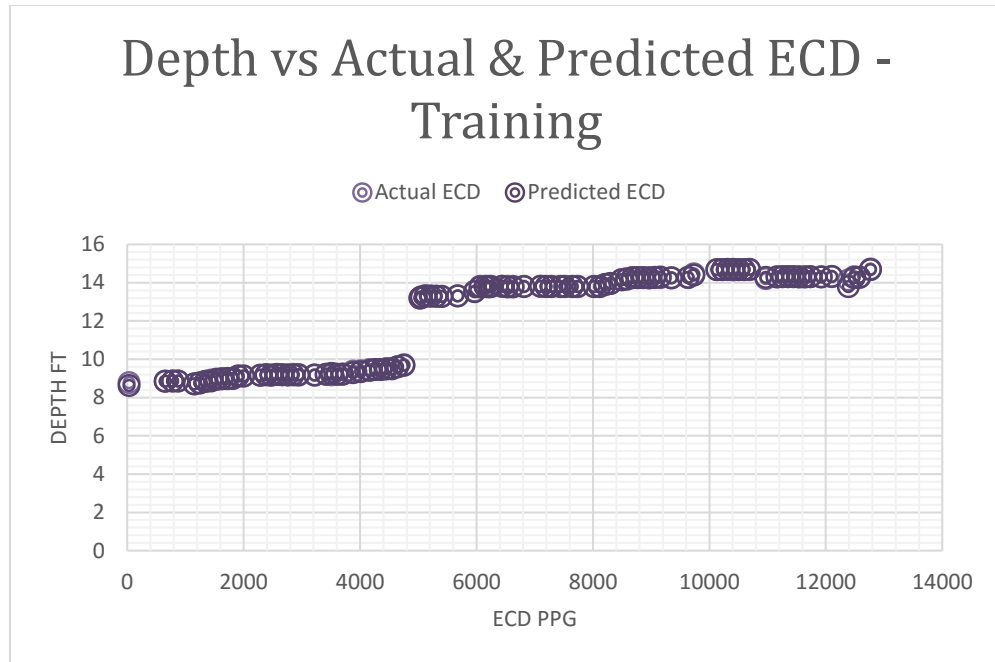


Figure 41 - ECD profile of training ANN model compared with ECD from field measurement

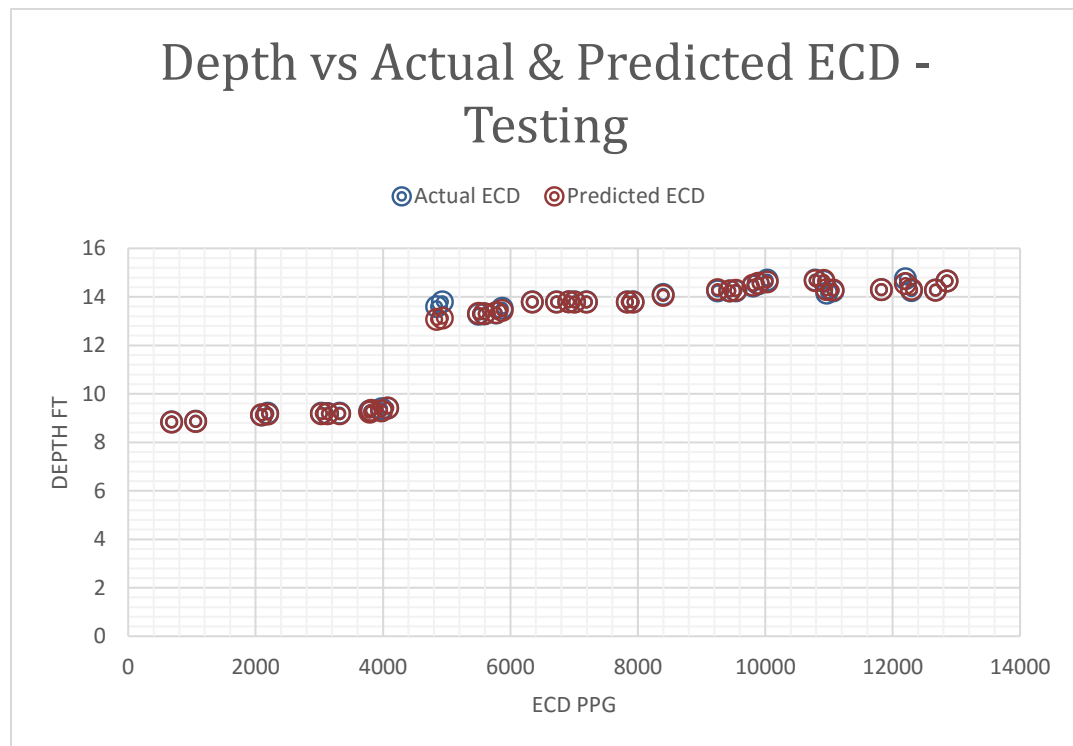


Figure 42 - ECD profile of training ANN model compared with ECD from field measurement

As expected, accurate results were obtained for real predicted ECD values. (**Table 12**) is showing the high accuracy using correlation coefficient and average absolute error percent (AAPE) as follows:

**Table 12 - ECD/ANN model training and testing Correlation Coefficient and AAPE**

Parameter	Training	Testing
Correlation Coefficient	0.9998	0.9980
Average absolute percentage error (%)	1.890	4.792

#### **4.1.2 Stage 2 - Rheological Properties Prediction**

AI ANN and ANFIS technologies had been used within this stage to predict real mud rheological parameters. High accuracy predicted values for yield point (YP), plastic viscosity (PV) and apparent viscosity (AV) will be used directly in the final HCI model. No need for lab measurements which takes time on the rig to measure these rheological variables.

An ANFIS model was created to predict drilling fluid yield point real values using 5 membership functions, using gaussmf as input membership function, and linear as output membership function with a random selection of training and testing data points. (**Figure 43**) and (**Figure 44**) shows the training and testing results for the required drilling fluid yield point values.

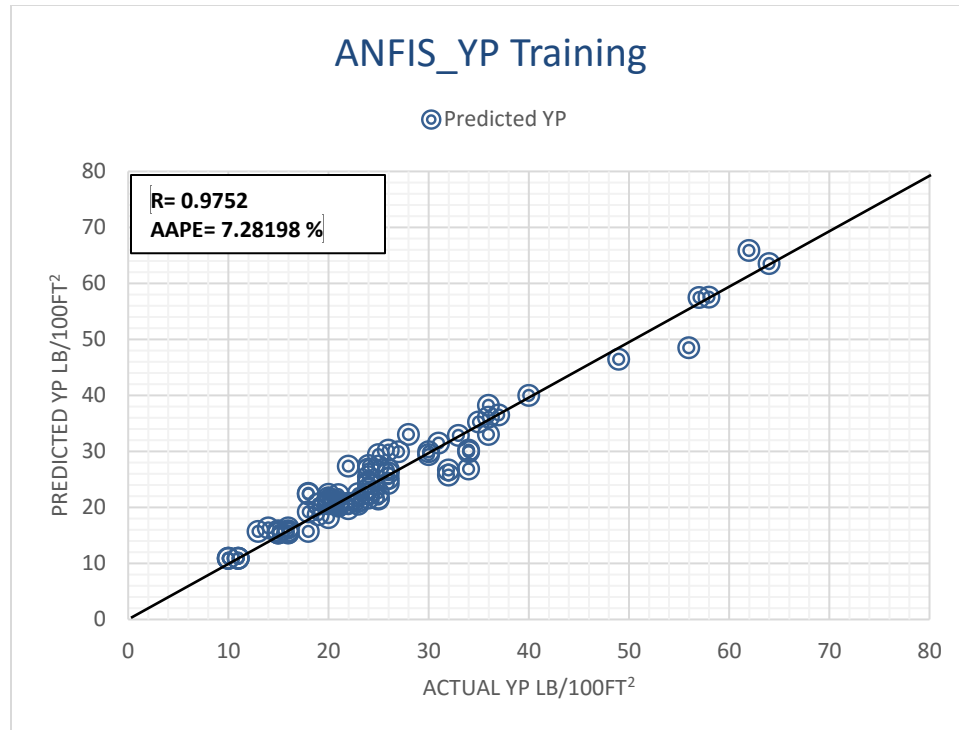


Figure 43 - Predicted YP from ANFIS Model compared with the field (training)

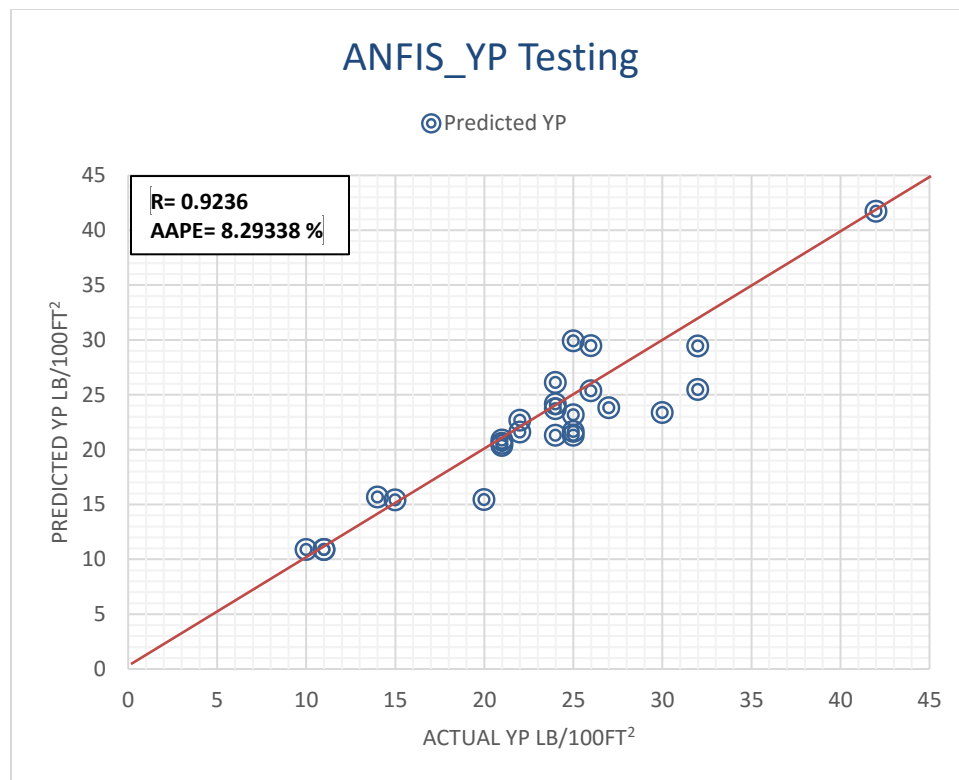


Figure 44 - Predicted YP from ANFIS Model compared with the field (testing)

Multiple layered neural network model was created with three layers to predict drilling fluid plastic viscosity and apparent viscosity. The 135 data points representing mud wt, funnel vis and solid volume as inputs were randomly used as following:

- 70% for training the network.
- 15% for testing the results.
- 15% to validate the network results.

(Figure 45) and (Figure 46) shows the training and testing results of predicting plastic viscosity values.

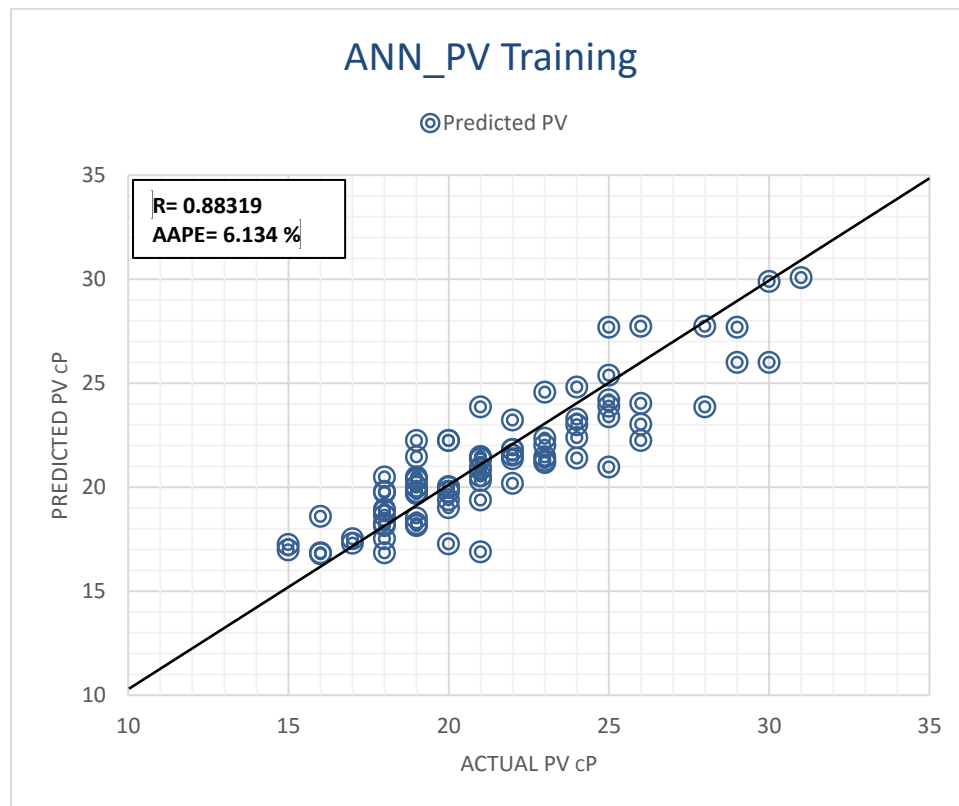
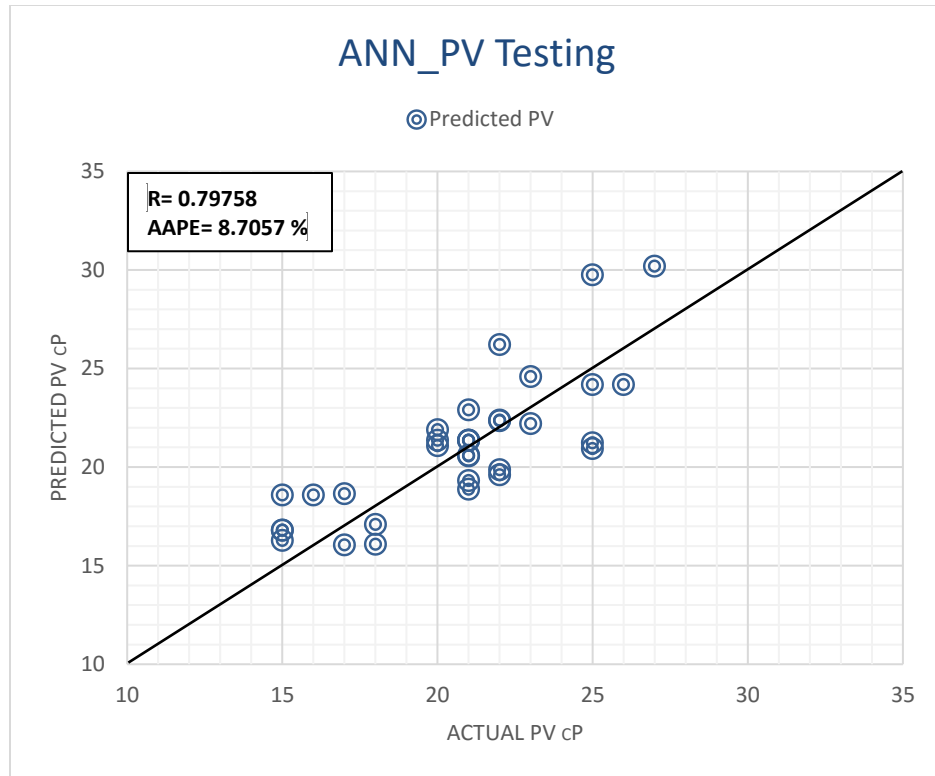


Figure 45 - Predicted PV from ANN Model compared with the field (training)





**Figure 46- Predicted PV from ANN Model compared with the field (testing)**

(Figure 47) and (Figure 48) shows the training and testing results of predicting apparent viscosity values.

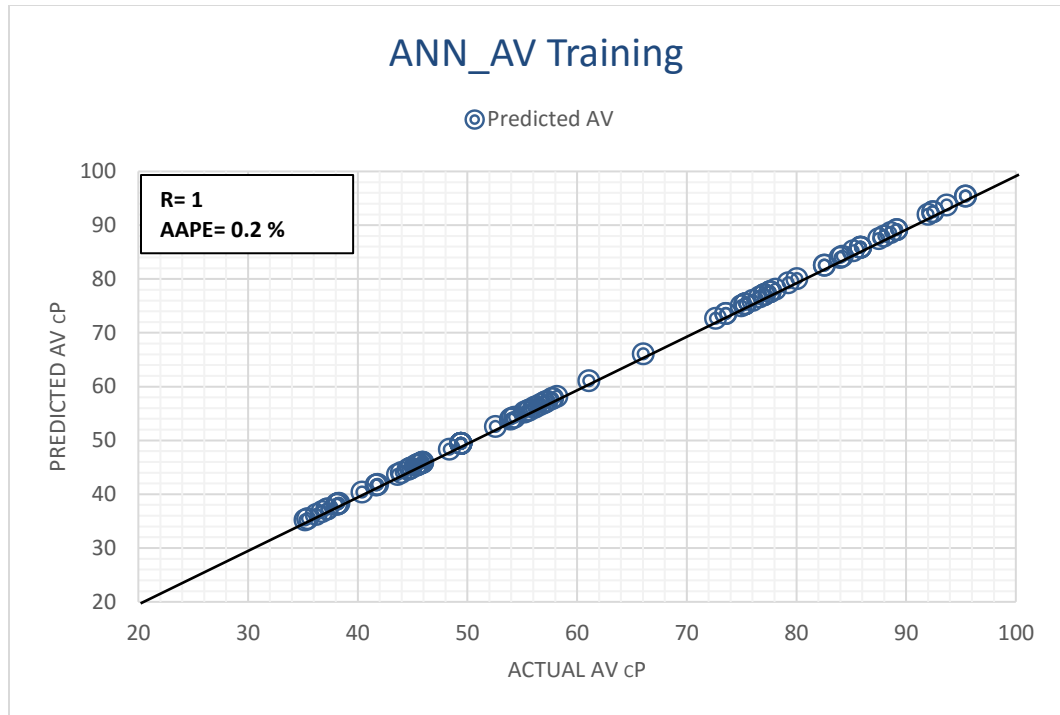


Figure 47 - Predicted AV from ANN Model compared with the field (training)

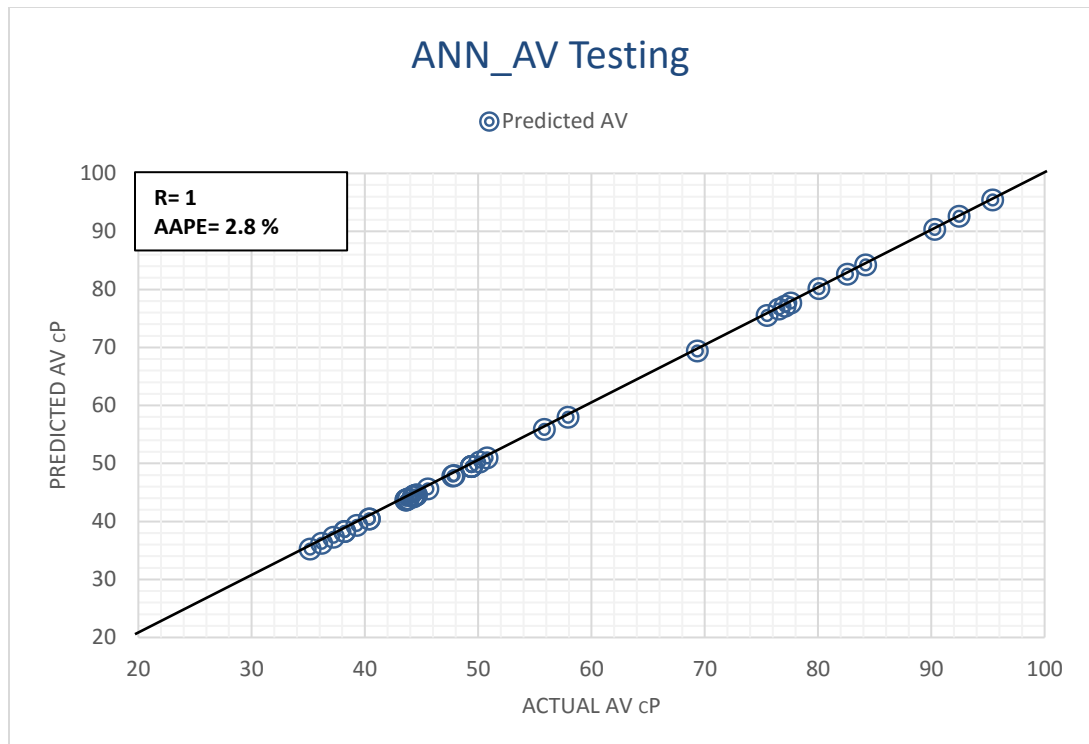


Figure 48 - Predicted AV from ANN Model compared with the field (testing)

High Accuracy results were obtained the real on-time developed AI rheological models. (Table 13) is showing the high accuracy using correlation coefficient and average absolute error percent (AAPE) as following:

**Table 13 - ANN & ANFIS rheological models training and testing Correlation Coefficient and AAPE**

Parameter	Correlation Coefficient (Training)	Correlation Coefficient (Testing)	Average absolute percentage error (%) - Training	Average absolute percentage error (%) - Testing
Yield Point (YP)	0.97	0.92	7.28	8.29
Plastic Viscosity (PV)	0.88	0.797	6.1	8.7
Apparent Viscosity (AV)	1	1	0.2	2.8

#### 4.1.3 Stage 3 – HCI Model Verification

The HCI model verification process has been done over several steps. Starting with developing the final HCI equation and working on its different variables' dimensions to match field and engineering concerns. The main aim from this model is to show the rig members on the surface what is happening regarding the hole cleaning condition downhole on-time. To achieve that HCI range classification was developed. This classification came basically from CCI initial equation. ([Drilling formulas Website](#)) provided two conditions of CCI good hole cleaning ( $CCI > 1$ ) and bad hole conditions ( $CCI \leq 0.5$ ). This initial approach was extended by the developed HCI model in this dissertation as follows:

- $HCI \geq 1$  (Good hole cleaning condition).
- $0.5 \geq HCI \leq 1$  (Bad hole cleaning condition – ROP to be decreased and shakers to be monitored on bottom ups).

- $HCI \leq 0.5$  (Stuck pipe situation – Immediate action should be taken – Stop drilling and circulate hole clean while working pipe up and down).

This approach will be tested and verified using the field case with 135 drilling data points. (Figure 49) shows how the drilling parameters became complicated starting from depth 8300 ft where the HCI model should give indications that there is bad hole cleaning to depth 12480 ft where the HCI model should give a high alert for stuck pipe conditions downhole.

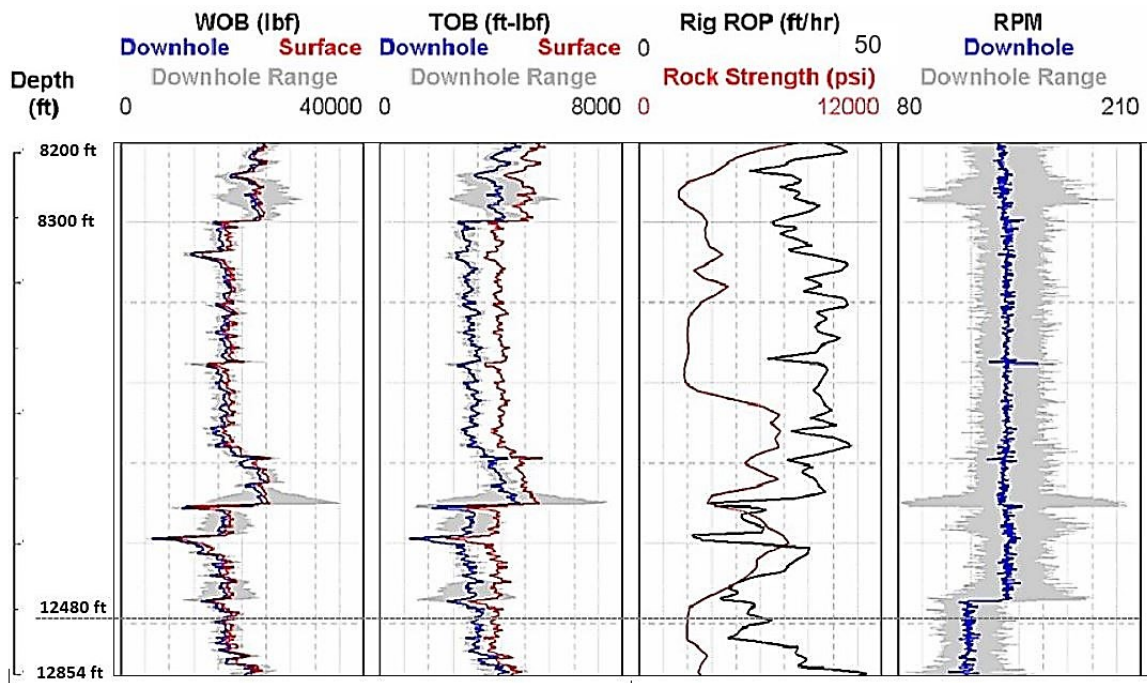


Figure 49 - Drilling parameters vs Depth – Showing hole cleaning conditions at depth of concern

By applying the 135 drilling data points with the developed HCI model, significant results were provided. (Table 14) is showing HCI values developed using predicted ECD and mud rheological values (YP, PV and AV).

Table 14 - HCI model outputs vs 135 depth points

Depth ft	HCI	Depth ft	HCI	Depth ft	HCI	Depth ft	HCI	Depth ft	HCI
32.8	7.854498699	3132.4	8.744285222	5405.44	10.92350559	7835.92	9.28376858	10410.72	0.651140094
656	6.43341777	3224.24	11.32812651	5500.56	7.768812202	7927.76	21.47853924	10505.84	0.614736522
685.52	8.313000168	3322.64	8.2765811	5592.4	10.68039332	8022.88	11.83098791	10597.68	0.79206937
780.64	6.737295361	3417.76	7.5541597	5680.96	10.46661746	8121.28	6.784137433	10692.8	0.754379921
875.76	7.475826355	3512.88	9.489476559	5776.08	8.094287754	8213.12	4.215864473	10787.92	0.958254045
1062.72	8.950562463	3604.72	8.782395325	5874.48	9.465137724	8304.96	0.618713021	10922.4	0.68028853
1157.84	9.580408746	3699.84	10.94181317	5969.6	6.937477216	8400.08	0.65620912	10968.32	0.766858287
1249.68	10.8650276	3791.68	10.87496557	6061.44	8.472717538	8495.2	0.890149382	10971.6	0.822823832
1348.08	12.79309158	3817.92	9.251192506	6153.28	17.79117602	8583.76	0.878957714	11066.72	0.559244856
1439.92	11.8096046	3883.52	9.89286866	6212.32	6.104405562	8678.88	0.916000531	11165.12	0.80544668
1535.04	8.370441645	3978.64	9.34400924	6251.68	5.482043983	8774	0.572875655	11260.24	0.99502048
1626.88	9.491923957	4014.72	8.41292725	6346.8	9.959304354	8869.12	0.570474622	11352.08	0.968527345
1722	8.069326478	4073.76	7.249752144	6441.92	6.991555856	8967.52	0.828189753	11447.2	0.553084802
1817.12	7.779443179	4168.88	8.122033421	6537.04	9.866642964	9065.92	0.880152425	11545.6	0.734658309
1908.96	7.548373607	4264	10.91032842	6632.16	8.44692578	9157.76	0.886409513	11640.72	0.741289598
2004.08	8.187234278	4359.12	9.47301446	6727.28	8.134073126	9256.16	0.965565336	11735.84	0.673151844
2095.92	9.570190595	4454.24	7.381078541	6819.12	8.758077914	9351.28	0.989438036	11827.68	0.614639896
2191.04	4.803761127	4549.36	8.203771858	6917.52	8.262376996	9446.4	0.856567605	11922.8	0.652153586
2286.16	10.69450956	4644.48	10.10107517	7009.36	9.547058741	9541.52	0.770199158	12106.48	0.580382837
2384.56	9.949087489	4756	9.718423437	7104.48	8.719412759	9636.64	0.601359449	12204.88	0.580382837
2476.4	10.04643906	4841.28	9.872659451	7193.04	21.75411697	9735.04	0.607848289	12296.72	0.98184477
2568.24	8.39474939	4936.4	10.15722039	7196.32	19.37337381	9810.48	0.906845469	12391.84	0.739078481
2663.36	9.952204754	5031.52	9.594550956	7291.44	26.36624568	9892.48	0.883455604	12486.96	0.356246804
2758.48	8.104959005	5054.48	9.737944509	7445.6	19.82910089	10033.52	0.772597898	12582.08	0.487824022
2853.6	12.11553361	5123.36	11.19320783	7517.76	12.86502952	10128.64	0.880882501	12677.2	0.479053745
2945.44	5.312110298	5215.2	10.37273743	7645.68	11.63039181	10223.76	0.78986064	12772.32	0.494746829
3037.28	7.123969274	5310.32	9.917561028	7740.8	15.42599225	10318.88	0.527244975	12854.32	0.387713328

The green cells are showing depths where HCI output values are higher than 1.0 which means good downhole cleaning conditions. Yellow intervals are showing depths drilling points where HCI output values are less than 1.0 and higher than 0.5, which means bad downhole cleaning conditions. The red cells are showing depth measurement intervals at which HCI model output values are less than 0.5. When HCI values are less than 0.5 this means that the downhole cleaning conditions are crucial and stuck pipe is seriously close to happening unless immediate actions being done from the rig crew to avoid it.

## **4.2 HCI Software**

The new hole cleaning model (HCI) which has been developed within this dissertation has results match the real drilling field scenario. At depths 12480 ft to 12485 ft the crew members faced erratic torque with differentiation in drilling parameters resulting in worst stuck pipe condition. To make it reliable, a software was developed based on the developed HCI model to give a visual alarm when HCI values are between 1.0 and 0.5 and visual with sound alarm when HCI values are lower than 0.5. **Figures 50, 51 and 52** are showing HCI model software at depth 1908 ft with good hole condition, depth 10692.8 ft with bad hole cleaning condition and depth 12854.32 ft showing critical hole cleaning condition resulting in downhole stuck pipe.

The screenshot shows the HCE Calculator application with the following input and output values:

Parameter	Value	Parameter	Value
PV	25	$\mu_a$	45.8
YP	26	$\Theta_{ang}$	24.97
ROP	52.48	D(50)	0.822
D(pipe)	5	ECD	67.99
D(hole)	16		

At the bottom, the calculated HCE value is 7.54627602779309, and the 'Stop Alarm' button is visible.

Figure 50 - HCI model calculator showing good hole cleaning at depth 1908 ft

The screenshot shows the HCE Calculator application with the following input and output values:

Parameter	Value	Parameter	Value
PV	19	$\mu_a$	75.34
YP	27	$\Theta_{ang}$	24.62
ROP	29.52	D(50)	0.798
D(pipe)	5	ECD	109.21
D(hole)	12.25		

The calculated HCE value is 0.7533456989270713. A 'Warning' dialog box is displayed with the message 'Bad hole cleaning' and an 'OK' button.

Figure 51 - HCI model calculator showing bad hole cleaning at depth 10692.8 ft

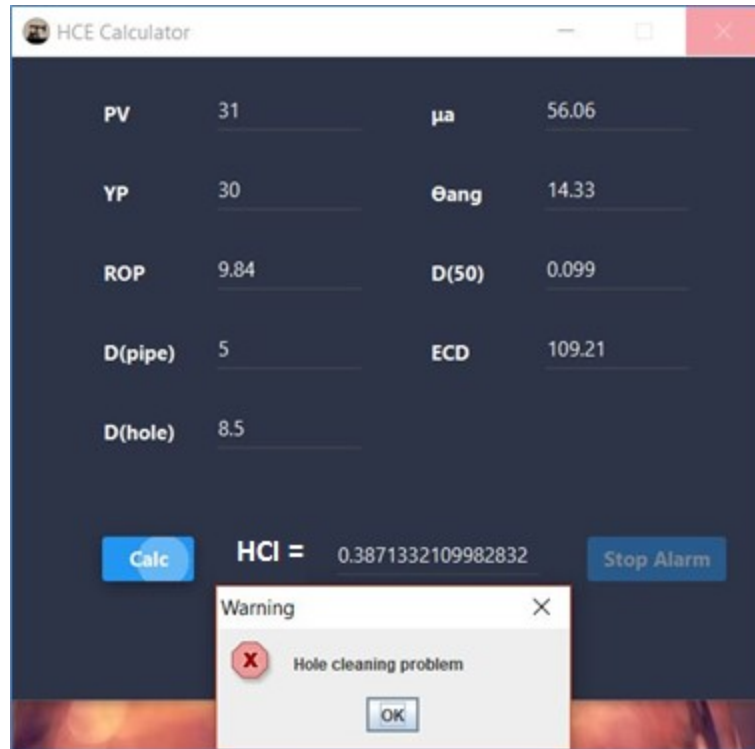


Figure 52 - HCI model calculator showing crucial hole cleaning (stuck pipe) at depth 12854.32 ft

### 4.3 Analysis and Limitations

Drilling oil wells – vertical, deviated or horizontal wells – is a blind process. Blindness comes from drilling downhole and lag time. Lag time is the delay between what is actually happening downhole and the notification of that on the surface. Drillers used to depend on their experience and ability to notice drilling trend parameters to judge the downhole cleaning conditions. Within this thesis, efficient hole cleaning model was developed to monitor downhole conditions while drilling in real-time. No need for downhole tools (e.g. MWD and LWD) to measure any of the model inputs. The alarm will be displayed on the driller monitor when bad or critical hole cleaning condition occur downhole.



Is that model applicable for all drilling data range? Till now it had been verified for one drilled oil well. The data being used as the model inputs – listed in chapter three – need to be measured on active wells for research purposes. Limitations for this model can be listed as follows:

- Rate of penetration (ROP) from 9.84 to 55.76 ft/hr.
- Particle size distribution (D50) from 0.1 mm to 3.72 mm.

The reason for using these two parameters as model limitations is their great impact on the model which is practically correct. From operational side of view, drillers and drilling engineers identify the hole cleaning by monitoring the shakers and its cutting capacity. Also, they control and enhance hole cleaning by controlling the rate of penetration while maintaining circulation.

#### **4.4 Conclusions**

The importance of monitoring the hole cleaning downhole while drilling is major to have efficient oil well drilling operations. Depending on the operators experience and shale shaker monitoring cannot be enough. Millions of dollars had been wasted on downhole cleaning problems. This dissertation provided a new model which can monitor the hole cleaning condition while drilling. The new model depends on surface drilling parameters which will skip the need for any downhole measurements.

Three models had been developed in this dissertation. The first model is an AI model which used ANN technology to predict ECD values while drilling from surface drilling data (ROP, Mwt in and DPP), which means no need for MWD downhole measurements. The second model is another AI model which used a combination of

ANFIS and ANN technologies to predict mud rheological properties (YP, PV, and AV) while drilling. The third model is a new hole cleaning identification tool (HCI) which used surface drilling parameters along with predicted ECD and rheological models' outputs to define the downhole cleaning condition on-time while drilling.

A software has been developed thru this dissertation to show the effective use of HCI model in the drilling industry. HCI indications can be used to avoid costly hole cleaning problems. It was proven that when drilling rigs cyber system be equipped with these three models, the driller will be able to monitor downhole cleaning conditions once happen without lag time to appear on the surface. This new technology will save millions USD for the drilling industry when being used effectively.

## References

- [1] A.Saasen."The Effect of Drilling Fluid Rheological Properties on Hole Cleaning", Proceedings of IADC/SPE Drilling Conference DC,02/2002
- [2] Al-Ajmi M, Abdulraheem A, Mishkhes A, and Al-Shammari M (2015) Profiling Downhole Casing Integrity Using Artificial Intelligence. In: The SPE Digital Energy Conference and Exhibition, The Woodlands, Texas, USA. SPE-173422-MS.
- [3] Alarfaj M, Abdulraheem A, and Busaleh Y (2012) Estimating Dewpoint Pressure Using Artificial Intelligence. In: The SPE Saudi Arabia section Young Professionals Technical Symposium, Dhahran, Saudi Arabia. SPE-160919-MS.
- [4] AliZakerian, Siyamak Sarafraz , Amir Tabzar, Nassim Hemmati, Seyed Reza Shadizadeh. "Numerical modeling and simulation of drilling cutting transport in horizontal wells", Journal of Petroleum Exploration and Production Technology, 2018
- [5] Al-Thuwaini J, Zangl G, and Phelps R (2006) Innovative Approach to Assist History Matching Using Artificial Intelligence. In: The Intelligent Energy Conference and Exhibition, Amsterdam, The Netherlands. SPE-99882-MS.
- [6] Andagoya K, Avellán F, and Camacho G, (2015) ECD and Downhole Pressure Monitoring While Drilling at Ecuador Operations. In: The SPE Latin American and Caribbean Petroleum Engineering Conference, Quito, Ecuador. SPE-177062-MS.
- [7] Ataga E, Ogbonna J, and Boniface O (2012) Accurate Estimation of Equivalent Circulating Density During High Pressure High Temperature (HPHT) Drilling Operations. In: Annual International Conference and Exhibition, Lagos, Nigeria. SPE-162972-MS.

- [8] Ayad A. Al-Haleem Abd Al-Razzaq, Abdul-Aali Dabbaj, Firas Mohammed Hadi. "Optimization of Hole Cleaning In Iraqi Directional Oil Wells ", Journal of Engineering, 2016
- [9] Babs Oyeneyin. "Multiphase Solids Transport", Elsevier BV, 2015
- [10] Baranthol C, Alfenore J, Cotterill M, and Poux-Guillaume G, (1995) Determination of Hydrostatic Pressure and Dynamic ECD by Computer Models and Field Measurements on the Directional HPHT Well 22130C-13. In: The SPE/IADC Drilling Conference, Amsterdam, Netherlands. SPE-29430-MS.
- [11] Bello O, Teodoriu C, Yaqoob T, Oppelt J, Holzmann J, and Obiwanne A (2016) Application of Artificial Intelligence Techniques in Drilling System Design and Operations: A State of the Art Review and Future Research Pathways. In: SPE Nigeria Annual International Conference and Exhibition, 2-4 August, Lagos, Nigeria. SPE-184320-MS
- [12] Bharambe M, and Dharmadhikari S (2016) Stock Market Analysis Using Artificial Neural Network on Big Data Minal Punjo Bharambe and S C Dharmadhikari. European Journal of Advances in Engineering & Technology. 3:26-33
- [13] Bybee K (2009) Equivalent-Circulating-Density Fluctuation in Extended-Reach Drilling. Journal of Petroleum Technology, 61: 64–67.  
<https://doi.org/10.2118/0209-0064-JPT>
- [14] Caicedo H, Pribadi M, Bahuguna S, Wijnands F, and Setiawan N (2010) Geomechanics, ECD Management and RSS to Manage Drilling Challenges in a Mature Field. In: The SPE Oil and Gas India Conference and Exhibition, Mumbai, India, 20-22 January. SPE-129158-MS.
- [15] Cho Hyun. "A Three-Segment Hydraulic Model for 71 words \_ < Cuttings Transport in Horizontal and Deviated Wells", Proceedings of SPE/CIM International Conference on Horizontal Well Technology ICHWT, 11/2000

- [16] Costa S, Stuckenbruck S, Fontoura S, and Martins A (2008) Simulation of Transient Cuttings Transportation and ECD in Wellbore Drilling. In: The Europec/EAGE Conference and Exhibition, Rome, Italy. SPE-113893-MS.
  
- [17] Daneshwar M, Noh N (2013) Adaptive neuro-fuzzy inference system identification model for smart control valves with static friction. In: Control System, Computing and Engineering (ICCSCE), IEEE International Conference, Mindeb, Malaysia.
  
- [18] Denney D (1998) Artificial-Intelligence Approach for Well-To-Well Log Correlation. Journal of Petroleum Technology. 50:30-32. SPE-1198-0030-JPT.
  
- [19] Diaz H, Miska S, Takach N, and Yu M (2004) Modeling of ECD in Casing Drilling Operations and Comparison with Experimental and Field Data. In: The IADC/SPE Drilling Conference, Dallas, Texas. SPE-87149-MS.
  
- [20] Dokhani V, Ma Y, and Yu M (2016) Determination of equivalent circulating density of drilling fluids in deepwater drilling. Journal of Natural Gas Science and Engineering. 34:1096-1105.
  
- [21] E. Kuru. "Hydraulic Optimization of Foam Drilling For Maximum Drilling Rate", Proceedings of SPE/IADC Underbalanced Technology Conference and Exhibition UTCE, 10/2004
  
- [22] E.GhasemiKafrudi, S.H. Hashemabadi. "Numerical study on cuttings transport in vertical wells with eccentric drillpipe", Journal of Petroleum Science and Engineering, 2016
  
- [23] Elkatatny S (2017) Real Time Prediction of Rheological Parameters of KCl Water-Based Drilling Fluid Using Artificial Neural Networks. Arabian Journal of Science and Engineering. 42:1655-1665

- [24] Elkatatny S, and Mahmoud M (2018a) Development of a New Correlation for Bubble Point Pressure in Oil Reservoirs Using Artificial Intelligent Technique. Arab J Sci Eng. 43: 2491-2500.
- [25] Elkatatny S, Mahmoud M., Mohamed I, et al. (2018b) Development of a new correlation to determine the static Young's modulus. J Petrol Explor Prod Technol. 8: 17–30
- [26] Erge O, Vajargah, A, Ozbayoglu M, and Van-Oort E. (2016) Improved ECD Prediction and Management in Horizontal and Extended Reach Wells with Eccentric Drillstrings. In: The IADC/SPE Drilling Conference and Exhibition, Fort Worth, Texas, USA. SPE-178785-MS.
- [27] Ettehad Osgouei R, Yoong S, and Ozbayoglu M (2013) Calculations of Equivalent Circulating Density in Underbalanced Drilling Operations. In: The International Petroleum Technology Conference, Beijing, China. IPTC-16601-MS.
- [28] Hacıislamoglu M (1994) Practical Pressure Loss Predictions in Realistic Annular Geometries. In: The SPE Annual Technical Conference and Exhibition, New Orleans, Louisiana. SPE-28304-MS.
- [29] Hamdan H, and Garibaldi J (2010) An investigation of the effect of input representation in ANFIS modelling of breast cancer survival. In: Proceedings of the International Conference on Fuzzy Computation and International Conference on Neural Computation, parts of the International Joint Conference on Computational Intelligence IJCCI, Valencia, Spain.
- [30] Hashemzadeh, Seyed Mohsen, and Ebrahim Hajidavalloo. "Numerical investigation of filter cake formation during concentric/eccentric drilling", Journal of Petroleum Science and Engineering, 2016.
- [31] Hemphill T, and Ravi K (2011) Improved Prediction of ECD with Drill Pipe Rotation. International Petroleum Technology Conference. In: The International Petroleum Technology Conference, Bangkok, Thailand. IPTC-15424-MS

- [32] Hemphill T, Bern P, Rojas J, and Ravi K (2007) Field Validation of Drillpipe Rotation Effects on Equivalent Circulating Density. In: The SPE Annual Technical Conference and Exhibition, Anaheim, California, U.S.A. SPE-110470-MS.
  
- [33] Hinton G, Osindero S, and Teh Y (2006) A fast learning algorithm for deep belief nets. *Neural Computation*, 18:1527-54.
  
- [34] Indra Gunawan. "Determining Cutting Transport Parameter in a Horizontal Coiled Tubing Underbalanced Drilling Operation", Proceedings of SPE Asia Pacific Oil and Gas Conference and Exhibition A POGCE, 10/2002
  
- [35] J. Li. "Sensitivity Analysis of Hole Cleaning Parameters in Directional Wells", Proceedings of SPE/ICoTA Coiled Tubing Roundtable CTR, 05/1999
  
- [36] Janjua I, Faizal SA, and Dabyah AA (2011) ECD Management in a Middle East well with the aid of Formation Pressure While Drilling. In: The SPE Saudi Arabia section Young Professionals Technical Symposium, Dhahran, Saudi Arabia. SPE-155414-MS.
  
- [37] Jeff Li. "Do Complex Super-Gel Liquids Perform Better Than Simple Linear Liquids in Hole Cleaning With Coiled Tubing?", Proceedings of SPE/ICoTA Coiled Tubing Conference and Exhibition CT, 04/2005
  
- [38] Jennifer Li. "Fluid Flow and Particle Transport Analyses Show Minimal Effect of Annulus Between Horizontal Wellbore and Expandable Screen", Proceedings of SPE Annual Technical Conference and Exhibition ATCE, 10/2005
  
- [39] Kien Lim. "Bit Hydraulics Analysis for Efficient Hole Cleaning", Proceedings of SPE Western Regional Meeting WRM , 05/1996

- [40] Kumar A (2012) Artificial Neural Network as a Tool for Reservoir Characterization and its Application in the Petroleum Engineering. In: The Offshore Technology Conference, Houston, Texas, USA. OTC-22967-MS.
- [41] Lei Zhou."Hole Cleaning During UBD in Horizontal and Inclined Wellbore", Proceedings of IADC/SPE Drilling Conference DC,02/2006
- [42] Lei Zhou."Hole Cleaning During Underbalanced Drilling in Horizontal and Inclined Wellbore", SPE Drilling & Completion, 09/2008
- [43] Liew S, Khalil-Hani M, and Bakhteri R (2016) An optimized second order stochastic learning algorithm for neural network training. *Neurocomputing*, 186:74-89
- [44] Lim, J, Kang J, and Kim J (1998) Artificial Intelligence Approach for Well-to-Well Log Correlation. In: The SPE India Oil and Gas Conference and Exhibition, New Delhi, India. SPE-39541-MS.
- [45] Lin T, Chenxing C, Zhang Q, and Sun T (2016) Calculation of Equivalent Circulating Density and Solids Concentration in The Annular When Reaming The hole in Deepwater Drilling. *Chemistry and Technology of Fuels and Oils*. 52:70–75.
- [46] Lippmann R (1987) An introduction to computing with neural nets. *IEEE ASSP Magazine*, 4:4-22.
- [47] Mehmet Ozbayoglu."Effect of Pipe Rotation on Hole Cleaning for Water-Based Drilling Fluids in Horizontal and Deviated Wells", Proceedings of IADC/SPE Asia Pacific Drilling Technology Conference and Exhibition APDT , 08/2008
- [48] M. E. Ozbayoglu."Critical Fluid Velocities for Removing Cuttings Bed Inside Horizontal and Deviated Wells", *Petroleum Science and Technology*, 04/2010



- [49] M.Green. "An Integrated Solution of Extended- Reach Drilling Problems in the Niakuk Field, Alaska :Part II- Hydraulics, Cuttings Transport and PWD", Proceedings of SPE Annual Technical Conference and Exhibition ATCE, 10/1999
  
- [50] M.N. Belavadi."Experimental Study of the Parameters Affecting Cutting Transportation in a Vertical Wellbore Annulus", Proceedings of SPE Western Regional Meeting WRM, 03/1994
  
- [51] Mingqm Duan."Critical Conditions for Effective Sand-Sized Solids Transport in Horizontal and High-Angle Wells", Proceedings of Production and Operations Symposium POS,03/2007
  
- [52] N.P. Brown."Cleaning Deviated Holes: New Experimental and Theoretical Studies",Proceedings of SPE/IADC Drilling Conference DC, 02/1989
  
- [53] Naganawa S, Sato R, Ishikawa M (2014) Cuttings Transport Simulation Combined with Large-Scale Flow Loop Experiment and LWD Data Enables Appropriate ECD Management and Hole Cleaning Evaluation in Extended-Reach Drilling. In: The Abu Dhabi International Petroleum Exhibition and Conference, Abu Dhabi, UAE. SPE-171740-MS.
  
- [54] Nakamoto P (2017) Neural Networks and Deep Learning: Deep Learning explained to your granny – A visual introduction for beginners who want to make their own Deep Learning Neural Network (Machine Learning). CreateSpace Independent Publishing Platform.
  
- [55] Nevio Moroni. "Pipe Rotation Improves Hole Cleaning and Cement-Slurry Placement: Mathematical Modeling and Field Validation", Proceedings of Offshore Europe
  
- [56] Niculescu S (2003) Artificial neural networks and genetic algorithms in QSAR. Journal of Molecular Structure, 622:71-83.

- [57] Olivares G, Quintero C, and Gimenez R (2012) Production Monitoring Using Artificial Intelligence. In: The SPE Intelligent Energy International, Utrecht, The Netherlands. SPE-149594-MS.
  
- [58] Omosebi A, Osisanya S, Chukwu G, and Egbon F (2012) Annular Pressure Prediction During Well Control. In: The Nigeria Annual International Conference and Exhibition, Lagos, Nigeria. SPE-163015-MS.
  
- [59] Osisanya S, and Harris O (2005) Evaluation of Equivalent Circulating Density of Drilling Fluids Under High Pressure/High Temperature Conditions. In: The SPE Annual Technical Conference and Exhibition, Dallas, Texas. SPE-97018-MS.
  
- [60] Owens, ."Parameter Estimation in Continuum Models", Computational Rheology, 2002.
  
- [61] Razi M, Arz A, Naderi A, (2013) Annular Pressure Loss while Drilling Prediction with Artificial Neural Network Modeling, European Journal of Scientific Research. 95:272–288.
  
- [62] Rommetveit R, Odegard SI, Nordstrand C, Bjorkevoll KS, Cerasi PR, Helset HM, Havardstein ST (2010) Drilling a Challenging HP/HT Well Utilizing an Advanced ECD Management System with Decision Support and Real-Time Simulations. In: The IADC/SPE Drilling Conference and Exhibition, New Orleans, Louisiana. SPE-128648-MS.
  
- [63] S.Walker."The Effects of Particle Size, Fluid Rheology, and Pipe Eccentricity on Cuttings Transport", Proceedings of SPE/ICoTA Coiled Tubing Roundtable CTR,04/2000
  
- [64] Saasen. "Hole Cleaning During Deviated Drilling - The Effects of Pump Rate and Rheology", Proceedings of European Petroleum Conference EUROPEC, 10/1998

- [65] Saggaf M, and Nebrija E (1998) Estimation of Lithologies and Depositional Facies from Wireline Logs. In: The SEG Annual Meeting, New Orleans, Louisiana. SEG-1998-0288.
  
- [66] Salaheldin Elkatatny, Zeeshan Tariq, Mohamed Mahmoud. "Real time prediction of drilling fluid rheological properties using Artificial Neural Networks visible mathematical model (white box)", Journal of Petroleum Science and Engineering, 2016
  
- [67] Salaheldin Elkatatny. "Application of Artificial Intelligence Techniques to Estimate the Static Poisson's Ratio Based on Wireline Log Data", Journal of Energy Resources Technology, 2018
  
- [68] Sayadia A, Monjezi M, Talebi N, Khandelwal M (2013) A comparative study on the application of various artificial neural networks to simultaneous prediction of rock fragmentation and backbreak. Journal of Rock Mechanics and Geotechnical Engineering, 5: 318-324
  
- [69] Seyed Sa'ed Bahramian, Amin Nabati, Ebrahim Hajidavalloo. "Effect of different rheological models on prediction of tri-cone bit pressure drop", International Journal of Oil, Gas and Coal Technology, 2018
  
- [70] Shahkarami A, Mohaghegh S, Gholami V, and Haghighat S (2014) Artificial Intelligence (AI) Assisted History Matching. In: The SPE Western North American and Rocky Mountain Joint Meeting, Denver, Colorado. SPE-169507-MS.
  
- [71] Shanmuganathan S, and Samarasinghe S (2016) Studies in Computational Intelligence: Artificial Neural Network Modelling. First edition, Springer International Publishing.
  
- [72] Shing J, and Jang R (1993) ANFIS: Adaptive-Network-based Fuzzy Inference Systems. In: IEEE Transactions on Systems, Man, and Cybernetics, 23:665-685.

- [73] Tahar Aita, Rafik Baouche, Kamel Baddari. "Neuro-fuzzy system to predict permeability and porosity from well log data: A case study of Hassi R-Mel gas field, Algeria", Journal of Petroleum Science and Engineering, 2014
- [74] Tamer Moussa, Salaheldin Elkatatny, Mohamed Mahmoud, Abdulazeez Abdulraheem. "Development of New Permeability Formulation From Well Log Data Using Artificial Intelligence Approaches", Journal of Energy Resources Technology, 2018
- [75] Tie Yan, Kelin Wang, Xiaofeng Sun, Shizhu Luan, Shuai Shao. "State-of-the-art cuttings transport with aerated liquid and foam in complex structure wells", Renewable and Sustainable Energy Reviews, 2014
- [76] V.C. Kelessidis. "Flow Patterns and Minimum Suspension Velocity for Efficient Cuttings Transport in Horizontal and Deviated Wells in Coiled-Tubing Drilling", Proceedings of SPE/ICoTA Coiled Tubing Conference and Exhibition CT, 04/2003
- [77] Vajargah A, Sullivan G, and Oort E (2016) Automated Fluid Rheology and ECD Management. In: The SPE Deepwater Drilling and Completions Conference, Galveston, Texas, USA. SPE-180331-MS.
- [78] Vipulanandan, C., and A. Mohammed. "Effect of 9 words  $\gamma$  nanoclay on the electrical resistivity and rheological properties of smart and sensing bentonite drilling muds", Journal of Petroleum Science and Engineering, 2015.
- [79] Wang Y, and Salehi S (2015) Application of Real-Time Field Data to Optimize Drilling Hydraulics Using Neural Network Approach. Journal of Energy Resources Technology, 137:62903-062903-9.
- [80] Wang, Y.M.. "An adaptive neuro-fuzzy inference system for bridge risk assessment", Expert Systems With Applications, 200805

- [81] Weiss W, Balch R, and Stubbs B (2002) How Artificial Intelligence Methods Can Forecast Oil Production. In: The SPE/DOE Improved Oil Recovery Symposium, Tulsa, Oklahoma. SPE-75143-MS.
  
- [82] Wiener J, and Moll B (1995) Predict permeability from wireline logs using neural networks. Petroleum Engineer International, 68:777-787.
  
- [83] Wiener J, Rogers J, and Moll B (1995) Predict permeability from wireline logs using neural networks. Petroleum Engineer International, 68:777-787.
  
- [84] Wright James. "An Economic Appraisal of Hole Cleaning Using Hydraulic Horsepower and Jet Impact Force", Proceedings of SPE Western Regional/AAPG Pacific Section Joint Meeting WRM, 05/2003
  
- [85] Wu, X, and Nyland E (1986) Well Log Data Interpretation using Artificial Intelligence Technique. In: The SPWLA 27th Annual Logging Symposium, Houston, Texas, 9-13 June. SPWLA-1986-M
  
- [86] Yun-kui Yan."Rheological study on natural heteropolysaccharide based drilling fluid", Journal of Central South University of Technology, 02/2007
  
- [87] Zarandi M, Avazbeigi M, Ganji B (2010) A Multi-Agent Expert System for Steel Grade Classification Using Adaptive Neuro-fuzzy Systems. Expert systems, Petrica Vizureanu (ED.), ISBN: 978-953-307-032-2, InTech.
  
- [88] Zhang, Feifei. "Numerical simulation and experimental study of cuttings transport in intermediate inclined wells.", Proquest ,2015.
  
- [89] Zhang, H, Sun T, Gao D, Tang H (2013) A New Method for Calculating the Equivalent Circulating Density of Drilling Fluid in Deepwater Drilling for Oil and Gas. Chemistry and Technology of Fuels and Oils. 49:430-438.

## Vitae

Name	:Mahmoud Nader Mahmoud Elzenary
Nationality	:Egyptian
Date of Birth	:2/8/1986
Email	:Mnader@aberdeendrilling.com
Address	:Prince Metib Road, An Nuzhah, Dammam 34251
Academic Background	<p>Bachelor in Petroleum Engineering – Suez University 2008.</p> <p>Published “New Approach to Evaluate the Equivalent Circulating Density (ECD) Using Artificial Intelligence Techniques” in Journal of Petroleum Exploration and Production Technology 2018.</p> <p>Published “New Technology to Evaluate Equivalent Circulating Density While Drilling Using Artificial Intelligence” in ATSE 2018 conference, SPE-192282-MS.</p>